Consolidating and Re-evaluating the Human Disc Nutrient Microenvironment

Emily E. McDonnell [1,2] and Conor T. Buckley [1,2,3,4*]

[1] Trinity Centre for Biomedical Engineering, Trinity Biomedical Sciences Institute, Trinity College Dublin, The University of Dublin, Dublin, Ireland

[2] Discipline of Mechanical, Manufacturing and Biomedical Engineering, School of Engineering, Trinity College Dublin, The University of Dublin, Dublin, Ireland

[3] Advanced Materials and Bioengineering Research (AMBER) Centre, Royal College of Surgeons in Ireland & Trinity College Dublin, The University of Dublin, Dublin Ireland

[4] Tissue Engineering Research Group, Department of Anatomy and Regenerative Medicine, Royal College of Surgeons in Ireland, 121/122 St. Stephen's Green Dublin 2, Ireland

*Corresponding author: Conor T. Buckley

E-mail address: conor.buckley@tcd.ie

Address: Trinity Centre for Biomedical Engineering, Trinity Biomedical Sciences Institute, Trinity College Dublin, Ireland

Telephone: +353-1-896-2061

Key words: degeneration; intervertebral disc; oxygen; glucose; pH; metabolism; in-silico

Running Header: Human disc nutrient microenvironment

Abstract

Background: Despite exciting advances in regenerative medicine, cell-based strategies for treating degenerative disc disease remain in their infancy. To maximise the potential for successful clinical translation, a more thorough understanding of the *in vivo* microenvironment is needed to better determine and predict how cell therapies will respond when administered *in vivo*.

Aims: This work aims to reflect on the *in vivo* nutrient microenvironment of the degenerating IVD through consolidating what has already been measured together with investigative *in-silico* models.

Materials & Methods: This work uses *in-silico* modelling, underpinned by more recent experimentally determined parameters of degeneration and nutrient transport from the literature, to re-evaluate the current knowledge in terms of grade-specific stages of degeneration.

Results: Through modelling only the metabolically active cell population, this work predicts slightly higher glucose concentrations compared to previous *in-silico* models, while the predicted results show good agreement with previous intradiscal pH and oxygen measurements. Increasing calcification with degeneration limits nutrient transport into the IVD and initiates a build-up of acidity; however, its effect is compensated somewhat by a reduction in diffusional distance due to decreasing disc height.

Discussion: This work advances *in-silico* modelling through a strong foundation of experimentally determined grade-specific input parameters. Taken together, pre-existing measurements and predicted results suggest that metabolite concentrations may not be as critically low as commonly believed, with calcification not appearing to have a detrimental effect at stages of degeneration when cell therapies are an appropriate intervention.

Conclusion: Overall, our initiative is to provoke greater deliberation and consideration of the nutrient microenvironment when performing *in vitro* cell culture and cell therapy development. This work highlights an urgency for robust experimental glucose measurements in healthy and degenerating IVDs, not only to validate *in-silico* models but to significantly advance the field in fully elucidating the nutrient microenvironment and refining *in vitro* techniques to accelerate clinical translation.

Introduction

For more than three decades lower back pain has remained the leading case of disability worldwide.[1] Despite this, conventional treatments continue to focus on alleviating painful symptoms, often with limited long-term efficacy, rather than treating the underlying cause of intervertebral disc (IVD) degeneration.[2,3] Degeneration typically manifests within the central nucleus pulposus (NP) and even early degenerative changes are deemed irreversible, before progressing outwards through the annulus fibrosus (AF) and entire intervertebral joint.[4,5] As a result, injectable cell-based therapies are being explored as early strategies, focusing on stimulating intrinsic repair and/or recreating the biochemical composition and structural integrity of NP tissue through the use of an appropriate cell-type and biomaterial carrier.[6,7] These regenerative approaches for IVD degeneration are still very much in their infancy, particularly at a clinical level, and with an aging and increasingly sedentary population we anticipate exciting developments in the next few decades.[8] However, to help improve future advances the research field requires a more thorough understanding of the NP nutrient microenvironment, how it changes with degeneration and how potential cell-based therapies will respond to the specific microenvironment into which they are administered. This not only has important scientific merit but also significant value for clinical translation as the avascularity and "hostile" nature of the IVD is often believed to be a key factor linked to high failure of prospective studies.[9–11]

Cells within the IVD rely on diffusion from blood vessels surrounding the AF and capillary buds in the vertebral bodies for nutrient and metabolite exchange.[12] Axial transport through the central region of the cartilage endplate (CEP) is the critical pathway for nutrient supply to the NP and inner AF, while more minor solutes (e.g. negatively charged sulphates) are predominately supplied via the AF route.[13–16] These diffusion distances and limited supply rates, together with the metabolic activity of the disc cells, naturally give rise to nutrient

gradient profiles and higher acidity levels than the surrounding plasma concentration.[17] Native NP cells have been shown to adapt to their microenvironment as well as altering expression of specific acid-sensing ion channels (ASICs) believed to be involved in sustaining local acidity.[18–21] However, the inherent microenvironment conditions may adversely affect the survival and regenerative capacity of administered cells. A number of studies have investigated the effect of "disc-like" conditions on potential cell sources such as mesenchymal stem cells (MSCs)[22–26], articular chondrocytes[27,28], and nasal chondrocytes.[29,30] Nevertheless, unity and harmony are needed across the research field on what are actually considered physiologically or even pathologically relevant culture conditions. For example, various studies employ culture medium consisting of one or two vastly different glucose concentrations; either 5.5 mM (1 g/L) or 25 mM (4.5 g/L). While incubators are commonly operated at oxygen levels of 5 or 20 $\%O_2$ in the disc field, some investigators have utilised ranges from 2 – 21 $\%O_2$. Importantly noting that the higher limit, for both nutrients, is considered supraphysiological within the vasculature system, let alone an avascular musculoskeletal tissue.[31,32] On the other hand, it is more established to delineate pH levels as a function of degeneration; with pH 7.1 often used to represent healthy, pH 6.8 being mild degeneration and pH 6.5 representing severe degeneration.[22–26,30] Although we regard this as an important advancement in considering the specific microenvironment of the target stage of degeneration *in vitro*, we believe the range may need to be re-evaluated in terms of its clinical relevance for cell-based regeneration.

Over 50 years ago, it was hypothesised that CEP calcification may trigger degeneration through impeding the passage of nutrients to NP cells.[13] Early studies have shown increased calcium deposition concomitant with aging and degeneration grade[33,34], as well as a correlation between the ease of nutrient transport and calcification.[35] More recently glucose transport impaired by the presence of calcium has been observed in *ex vivo* organ cultures.[36] Increasing levels of calcium appears to diminish collagen and PG synthesis, and thus may impede solute diffusion

through adversely impacting tissue hydration.[36,37] The hypothesis of calcification as a degenerative trigger is supported by early *in vitro* studies where limited nutrient supply has reduced cell viability and functionality[38–42], while more recent work has explored the effects of additional matrix constituents impeding solute uptake.[43,44] For example, one study directly investigating solute diffusivity through cadaveric human CEP tissue (38 – 66 years) found significant variation in diffusion, with the least permeable CEPs having lower aggrecan, collagen-2, and MMP-2 gene expression.[43]

In addition to assessing cell functionality under limited nutrition and acidity, studies have used these adjusted culture concentrations as a priming strategy to support survival and enhanced extracellular matrix (ECM) deposition under harsher microenvironments.[45–47] These studies are preliminary *in vitro* investigations and *in vivo* studies must be performed to further consolidate the efficacy of priming. Another method is preconditioning to improve cell differentiation into native phenotypes within the diseased microenvironment.[11] Hypoxic preconditioning of MSCs demonstrated promising results pre-clinically[48,49], while human NP cells preconditioned at 2 %O_2 in a proprietary cocktail have progressed clinically to phase I/II trials (NCT03347708).[50,51]

While significant advances have been made in developing cell-based regeneration strategies[52,53], these exciting therapies have shown mixed results in terms of IVD regeneration.[54–56] Cell-based regeneration is contingent on cells remaining viable and maintaining their regenerative response under an exacerbated nutrient deficit.[9,11,57,58] In total, 16 clinical trials investigating cell-based therapies have been registered worldwide for IVD degeneration and although they demonstrate the procedures to be safe, clinical evidence of positive efficacy remains unclear.[8,54,55,59,60] To fully realise these strategies and maximise clinical translation of cell-based therapies, there is an urgent need to consolidate what is already known regarding the *in vivo* nutrient microenvironment.

Human disc nutrient microenvironment

A number of early studies have measured metabolite (glucose, lactate and oxygen) concentrations in animal discs.[14,61–63] However, their physiological relevance to the human IVD continues to be an area of debate, for example: geometrical scale, nutrient supply, species-specific differences in cells and metabolic rates, not to mention differences in aging and pathophysiological effects.[64] Given the inherent complexity of the IVD and difficulty in obtaining *in vivo* measurements, the research field is fortunate to avail of two seminal studies investigating intradiscal pH and oxygen in patients suffering from pathological backpain.[65,66] To the best of the authors' knowledge, only one study has experimentally investigated the human glucose microenvironment through enzymatic analysis of digested human tissue.[67] Unfortunately, from a quantitative perspective, normalised results were presented (e.g. relative to the IVD concentration at the apex of the scoliotic curvature) and do not provide further insight into the glucose concentrations *in vivo.* As a result, *in-silico* modelling acts as a complementary approach and a valuable tool to providing insights into the *in vivo* glucose concentrations. Schmidt *et al.* (2013) have compiled a comprehensive overview of *in-silico* models for IVD investigation[68], highlighting a number of nutrient transport models elucidating the metabolite concentrations in both healthy and degenerated IVDs.[69–77]

By gathering the results from the aforementioned literature, the current knowledge of the human nutrient microenvironment is consolidated in Figure 1. The exact location of NP glucose concentrations extracted from the *in-silico* studies is highlighted in Figure 1A and the range of predicted concentrations are presented in Figure 1B all of which will be discussed in more detail later. Figure 1A also highlights the direction of experimental measurements: Nachemson (1969) measured the intradiscal pH in 31 patients using a custom-made needle electrode introduced through a posterolateral approach[65,78], while Bartels *et al.* (1998) measured the oxygen profile in 13 patients suffering from scoliosis and 11 suffering from back pain using an anterior approach.[66] The full range of intradiscal pH measurements were between

5.7 and 7.5, with no significant difference between discs with prolapses (6.6 - 7.5) and those without visible pathologies (6.8-7.4). To re-evaluate these measurements with respect to potential cell-therapy intervention stage, the results from this early study are re-graphed in Figure 1C according to perceived pain level (see Methods section for details). Lumbar oxygen profiles for patients suffering from back pain are presented in Figure 1D, as they are a relevant cohort with respect to this work. However, the authors did observe considerable variability in oxygen among the lower back pain cohort and no correlation was determined between oxygen level and age or stage of degeneration. The metabolite profiles and concentrations presented in Figure 1 will be discussed in greater depth and re-evaluated with respect to cell-based regeneration throughout this article.

In summary, in this work we aim to reflect on early measurements of the *in vivo* nutrient microenvironment. Using *in-silico* modelling, underpinned by more recent experimentally determined parameters of degeneration and nutrient transport, we seek to re-evaluate the current knowledge in terms of grade-specific stages of degeneration. Focusing on the effect of considering a metabolically active cell population and grade-specific CEP calcification on the nutrient microenvironment and their implications for cell-based regeneration. Together we aim to provoke greater deliberation and consideration of the nutrient microenvironment when designing *in vitro* cell culture experiments and cell therapy development.

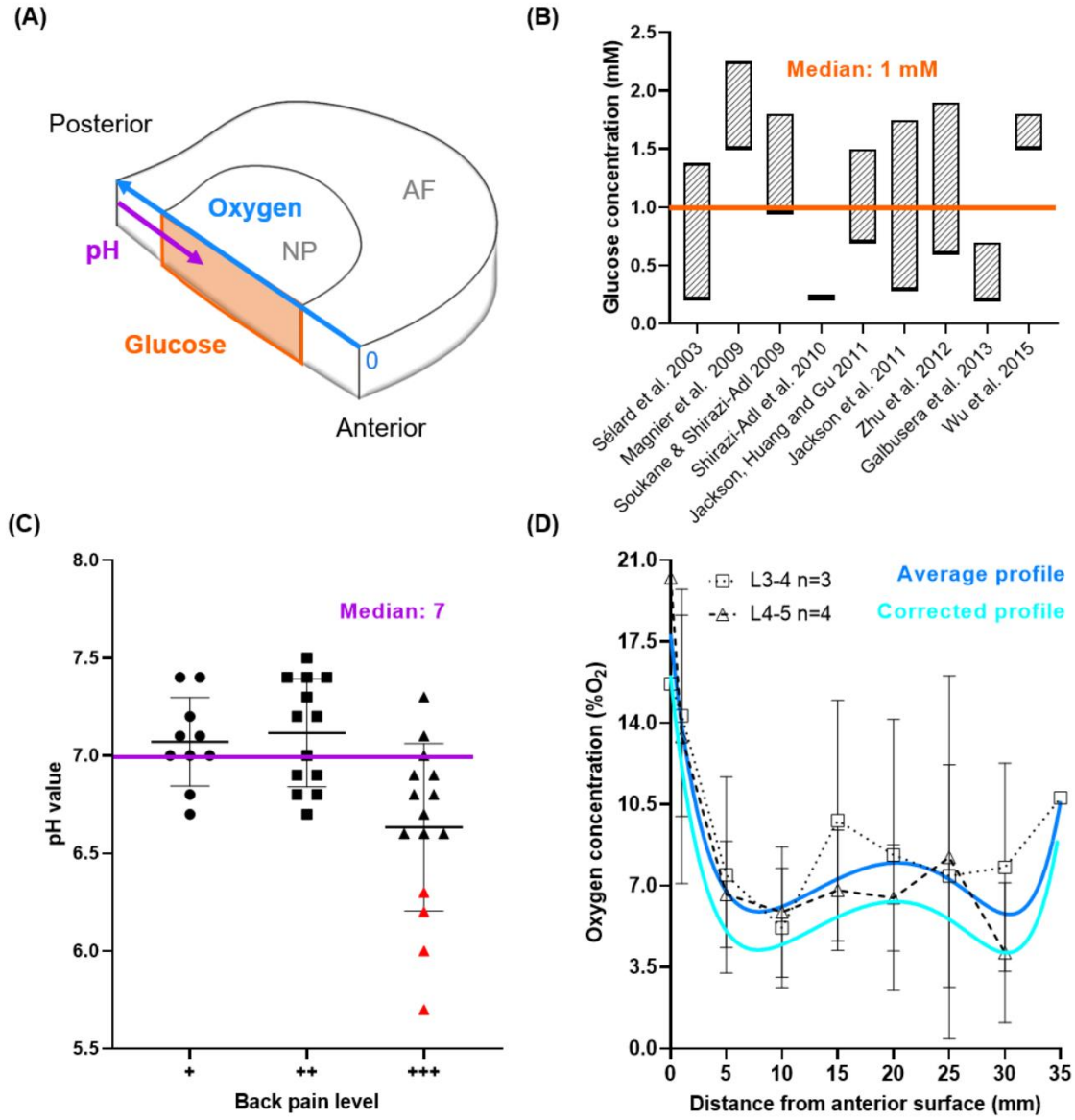

Figure 1. (A) A quadrant of a human intervertebral disc (IVD) indicating the location of predicted glucose, experimental pH and oxygen values. (B) A range of glucose concentrations predicted in a degenerated human IVD from *in-silico* models over the last 20 years. A median concentration of 1mM is highlighted across all studies. (C) The pH level in lumbar IVDs of patients experiencing different levels of back pain, extracted from Nachemson (1969). Data points highlighted in red included details of severe visible degeneration and were excluded from the calculated median as they are considered too late stage for regeneration through cell therapy. (D) Oxygen measurements by Bartels *et al.* (1998) from patients suffering from back pain were pooled based on their lumbar level and an average profile was fit using non-linear regression. A corrected predicted profile to account for elevated oxygen inhalation during surgery was determined using an *in-silico* model (Supplementary material).

Materials & Methods

Re-evaluating the nutrient microenvironment of the human IVD

NP glucose concentrations were extracted from nutrient transport models developed over the last two decades and a median value of 1 mM was calculated (Figure 1B) across these studies.[69–77] Intradiscal pH measurements from Nachemson (1969) were graphed based on the level of perceived pain (Figure 1C) and a median of pH 7 was calculated across the three categories of pain. It is important to note that four measurements in group +++ (red), with severe tissue granulation, scarring and adhesions were excluded as they are considered beyond the intervention stage for regeneration through cell therapy.[6]

Lumbar oxygen profiles extracted from Bartels *et al.* (1998) were pooled by lumbar level (7 donors; three L3/4 and four L4/5) and the profile was plotted as the mean ± standard deviation. One profile (CS-48yF-L4/L5) was excluded as the intradiscal concentrations were higher than the boundary concentration. Values were converted from partial pressure (mmHg) to $\%O_2$, using an approximate conversion table.[31] An average lumbar profile was created using a non-linear least squares curve fit (Figure 1D). It is important to acknowledge that the patients inhaled 30 $\%O_2$ for at least one hour during surgery as part of general anaesthesia. Although the authors postulate that this should not significantly alter concentrations beyond 5 mm from the AF disc surface, the main supply route to the NP through the CEP was not considered. Taking observations from a canine study investigating the response time for changes in arterial and intradiscal concentration after alternating the $\%O_2$ of inspired air[63], a time-dependent *in-silico* model was performed with an elevated boundary condition in order to predict a corrected oxygen profile (Supplementary Figure S1).

Compiling metabolite diffusion coefficients for intervertebral disc sub-tissues

Several studies have characterised glucose diffusivity in the NP, AF and CEP of both human IVDs and bovine discs.[79–83] However, many of the values reported are apparent diffusion

coefficients, while it is the intrinsic diffusivity or effective diffusion coefficient which is necessary for *in-silico* modelling. Based on statistical insignificance observed by the work of Jackson *et al.* (2012), a strain independent CEP partition coefficient was used to convert reported apparent coefficients to approximated effective glucose and lactate diffusion coefficients.[82,83] Where diffusion coefficients were determined at room temperature, the values were temperature corrected by using relative diffusivity in an aqueous solution.[81] Effective glucose diffusion coefficients in IVD tissue at 37°C are presented in Figure 2A, highlighting diffusional direction (AF), anatomical location (CEP) and the applied strain condition. The percentage change in effective glucose diffusion due to increasing applied strain was calculated and plotted in Figure 2B for NP, AF, and CEP. As measurements for lactate diffusion through NP and AF tissue are rare in the literature, the values presented in Figure 2C are estimated from experimental glucose diffusion using the relative diffusivity between glucose and lactate in aqueous solution. The percentage change in effective lactate diffusion due to increasing applied strain was calculated and plotted in Figure 2D for NP, AF, and CEP. In Figure 2E effective oxygen diffusion coefficients in both bovine and human AF were corrected for temperature as mentioned previously.[81,84] To the best of our knowledge, oxygen diffusion has not been experimentally measured in NP and CEP tissue. Therefore, theoretically calculated oxygen diffusion coefficients are presented[14], accompanied by typical values for cartilaginous tissue.[85–87] Due to the limited oxygen data, the percentage change in oxygen diffusion due to increasing applied strain could only be calculated for the AF, Figure 2F.

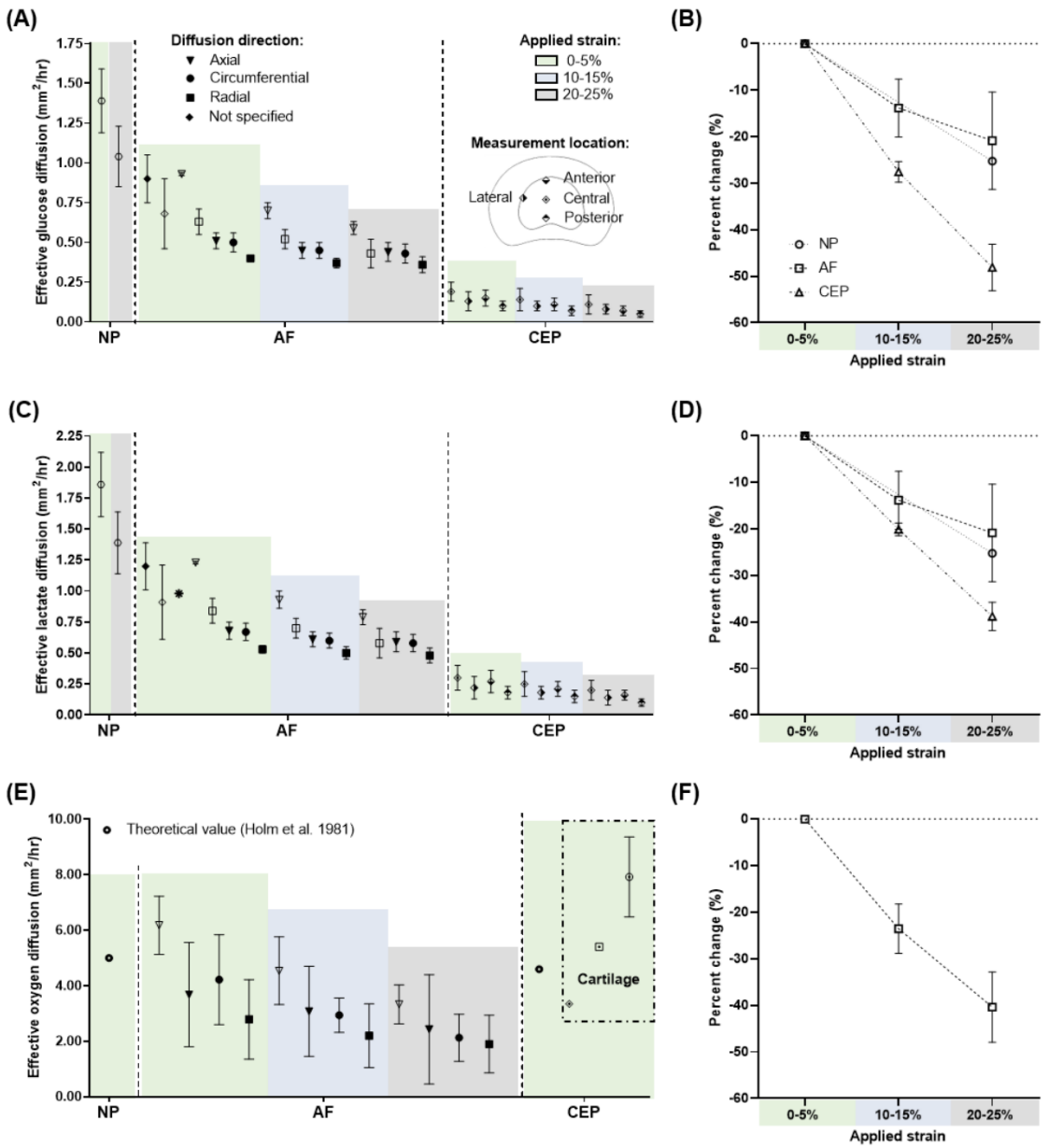

Figure 2. (A) Effective glucose diffusion through nucleus pulposus [79] (NP), annulus fibrosus [79–82] (AF) and cartilage endplate (CEP) tissue [88]. Experimental measurement conditions such as directionality through the anisotropic AF, applied strain for each tissue domain and measurement location within the CEP are highlighted. NP & AF: solid = human, outline = bovine. CEP: all human. (B) Change in glucose diffusivity due to applied strain for the two recorded strain levels in NP and three levels in both AF and CEP. (C) Effective lactate diffusion for NP and AF were estimated from the above glucose diffusion using relative diffusivity, while CEP values were experimentally measured.[88] (D) Change in lactate diffusivity due to applied strain for the two recorded strain levels in NP and three levels in both AF and CEP. (E) Theoretical calculations of effective oxygen diffusion in the NP and CEP have been reported [14], while AF values have been experimentally measured.[80,81] Values for oxygen diffusion in cartilage

are also included for comparison.[29,85,87] (F) Change in oxygen diffusivity due to applied strain within AF only, data subjected to different applied strains are not available for NP and CEP tissue.

Identifying experimental degeneration grade-dependent input parameters for in-silico models

In this work we are defining Grade II as healthy adult, Grade III as mild degeneration and Grade IV as moderate degeneration, while Grade V is considered too severe a stage of degeneration for regeneration using cell therapies.[10,57]

Total cell density values were taken from a study which investigated degeneration-related variation in cell density using H&E staining and Histological Degeneration Score (HDS) to grade 49 lumbar IVDs (22 donors) from Grade I-IV.[89] A more recent study determined the active or viable percentage of the NP and AF cell population by counting the proportion of cells stained positively for the formazan product of the 3-(4,5-dimethylthiazol-2-yl)-2,5-diphenyl-tetrazolium bromide (MTT).[90] The Pfirrmann scale was used to classify the degenerative status of two groups: Middle-aged (35-50 years) and Old-aged (>80 years). All 15 IVDs in the Middle-aged group were Grade I-III and all 13 IVDs in the Old-aged group were Grade IV or V. As a result, we created an active Criteria 1 (Middle-aged) to apply to total cell densities from Grade II & III and Criteria 2 (Old-aged) to apply to total cell densities from Grade IV. The percentage of active AF cells was averaged over the anterior and posterior regions. As there was no significant difference between the active criteria of NP and AF, we assumed an average active percentage to apply to the CEP cells (values shown in Figure 4A-6A). Figure 3A-C presents the total cell density from Liebscher *et al.* (2011) and an estimated active cell density after applying the relevant criteria from Martins *et al.* (2018)) across the IVD tissue and grades of degeneration. The exact numbers used as input parameters for the cell density of the grade-specific in-silico models can be found in Supplementary Table S2.

Human disc nutrient microenvironment

A 3-D model geometry was created using published dimensions for a human L4/L5 IVD.[91] While the anterior to posterior (A-P) and lateral width was assumed to remain constant, disc height was reduced with degeneration, Figure 3D. Disc height was determined using ImageJ analysis on macroscopic images of sagittal sections of lumbar IVD: average values for Grade II = 11.5 mm, Grade III = 8.8 mm and Grade IV = 6.7 mm.[92] For simplification the model is presented as a symmetrical quadrant of the full IVD, as highlighted in Figure 3D with each distinct tissue domain allocated its own cell density (only active is shown). Although an anatomically accurate CEP is explicitly modelled[93], it is not shown for easier interpretation of the results within the NP, and further details can be found in Supplementary Figure S3.

Mean hydration values were extracted from experimental studies which provided detail on degenerative appearance or grade and age as well as standard deviation and sample size. All extracted values are presented in Figure 3E-G, together with an overall mean hydration for each grade, calculated by combining the summary statistics across studies.[94] NP hydration incorporated four studies[95–98], with two providing values for two or more grades of degeneration.[95,98] AF hydration incorporated six studies, two of which were additional to those reported for NP.[99,100] Lyons *et al.* (1981) presented a hydration profile through "healthy" and "degenerated" discs. We split this profile into NP and AF and the average taken within those regions. Based on the adult age of the "healthy" group it was assigned to our Grade II and since the "degenerated" group underwent spinal fusion it was assumed to be at least Grade IV. Iatridis *et al.* (2007) presented their values for Grade II (n=2) and Grade III (n=7) combined. However, the authors stated that both grades displayed degeneration while Grade I was classified as "healthy" with no indication of age. Taking this into account as well as the higher proportion of Grade III samples we considered it most applicable for our Grade III definition. CEP hydration incorporated four studies[93,101–103], two of which provided values for two or more grades of degeneration.[93,101] Where values were presented separately for different anatomical

regions within tissue type e.g. anterior/posterior AF or superior/inferior CEP, an overall average was calculated for each study.[95,96,100]

As studies have shown ~10% strain under axial compression simulates physiological weightbearing[104–106], effective diffusion coefficients at 10-15% strain were used in the *in-silico* model. Where NP diffusion was only available for 0-5% and 20-25% strains (Figure 2), a midpoint was taken. Reduced NP hydration with degeneration (Figure 3E) was incorporated by decreasing the diffusion coefficients accordingly between Grades II, III and IV. Anisotropic diffusion in the AF was captured with lowest diffusivity in the radial direction and highest axially. Diffusion parameters through the central zone of the CEP were chosen as the zonal differences were relatively small and it is believed that the central region of the CEP is the predominant transport route to the NP.[13–15] With no clear trend between hydration and degeneration in the AF and CEP (Figure 3F,G), the solute diffusion coefficients were maintained constant. However, in the case of modelling the effect of CEP calcification on metabolite concentrations, diffusion through the CEP was reduced in accordance with the increase in calcium deposition. Calcification values of 15% for Grade II, 34% for Grade III and 58% for Grade IV were extracted from a study investigating the percentage of calcified tissue and Thompson degeneration classification in 60 cervical IVDs.[107] Diffusion through the CEP reduces in accordance with an increase in calcium deposition. As a result, the effective diffusion coefficients were reduced according to the increase in percentage of calcification between grades of degeneration. The finalised effective diffusion coefficients of glucose, lactate and oxygen through the different tissue domains are presented in Figure 3H-J and in Supplementary Table S4.

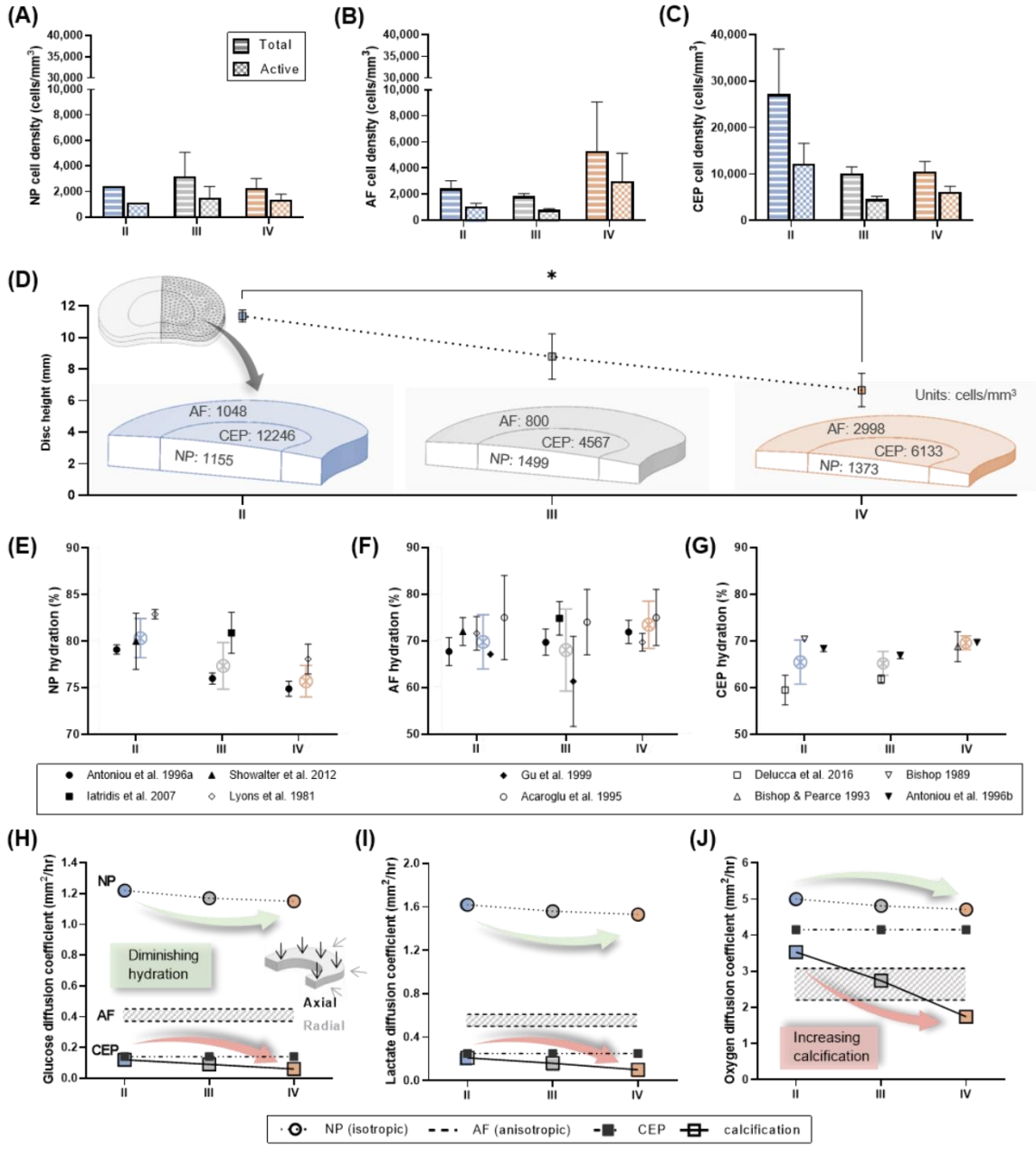

Figure 3. *In-silico* input parameters gathered from experimental literature. (A-C) Total and active cell density for the nucleus pulposus (NP), annulus fibrosus (AF) and cartilage endplate (CEP). The total values were extracted directly from a study by Liebscher *et al.* (2011), while the active density was extrapolated by applying an active criterion.[90] (D) Disc height as a function of degeneration determined through image analysis of sagittal lumbar IVD sections.[92] Inlay of model geometry which represented a quadrant of a human L4/L5 IVD with an active cell density for each tissue domain highlighted (cells/mm^3). (E-G) Tissue hydration as a function of degeneration grade obtained from the literature for NP, AF and CEP. An overall mean tissue hydration was calculated and highlighted (colour) by combining the summary statistics across studies. (H-J) Finalised glucose, lactate, and oxygen diffusion coefficients used in the in-silico model. NP diffusivity reduces with diminishing hydration; anisotropic

AF diffusion is captured within the shaded range, with higher diffusivity in the axial direction and lower in the radial direction; CEP diffusivity reduces in the presence of calcification.

Establishing in-silico models as a function of degeneration grade

The *in-silico* nutrient transport model was created using COMSOL Multiphysics 5.6 (COMSOL Inc., Burlington, USA). The steady-state nutrient microenvironment was governed by coupled reaction-diffusion equations accounting for the total or metabolically active cell density and metabolite diffusion parameters through the different tissue domains, specific to degeneration grade. Briefly, the metabolic rates (nutrient consumption and metabolite production) were modelled as being dependent on local pH and oxygen concentration by employing Michaelis-Menten equations.[108–111]An explanation of the equation coupling, and computational methodology can be found in our previous work, together with successful experimental validation, for intact bovine discs in ex vivo organ culture.[112] Michaelis-Menten constants for NP cells (V_{max} = 12 nmol/x10^{6}cells/hr and K_m = 12 µM) and AF cells (V_{max} = 8.6 nmol/x10^{6}cells/hr and K_m = 40 µM) were taken from experimental literature considered to be the most representative of the *in vivo* microenvironment in terms of maintaining a 3-D freshly isolated cell phenotype and physiologically relevant glucose concentrations.[109,110,113] With limited data available for CEP cells, values were obtained from culture expanded cells in suspension (V_{max} = 14.1 nmol/x10^{6}cells/hr and K_m = 15 µM).[114] Similar to previous numerical models[69–71], it was assumed that glucose and oxygen concentrations at the disc boundary are that of blood plasma in the surrounding blood vessels, 5.33 mM[32] and 12.6 %O_2[63], respectively. Holm et al. (1981) measured an oxygen concentration ~ 9.3 % O_2 in the vertebral bodies close to the CEP. A typical blood plasma pH of 7.35 – 7.45 was converted to lactate using a linear conversion and assumed constant at the AF and CEP boundaries.[109]

Investigating the optimal cell number for intradiscal injection

To identify an optimal cell number for intradiscal transplantation we used the active and calcified *in-silico* models for Grade II and IV. 3, 6, 9 and 18 million cells were investigated based on parameters of ongoing clinical trials from Mesoblast Ltd. (NCT01290367 & NCT02412735) and DiscGenics Inc. (NCT03347708). Cells were assumed to be homogeneously distributed throughout the NP, remain viable after delivery, and possess a discogenic phenotype, thus having similar metabolic rates and nutrient couplings as native NP cells.

Results

The developed *in-silico* models predict the relationship between metabolite concentration and the previously determined tissue properties of healthy adult (Grade II), mildly (Grade III) and moderately degenerated (Grade IV) human IVDs. The results are presented in the form of contour plots of just the lower quadrant of the disc, the concentration profile from anterior to posterior at mid-height through the disc, the centre most value in the NP and the percentage change in concentration due to the different conditions investigated e.g. active cell criteria and CEP calcification. These results are grouped by metabolite with glucose shown in Figure 4, pH in Figure 5 and oxygen in Figure 6.

As expected for a large avascular structure, the results showed that nutrient concentration decreases with distance from the blood supply at the disc periphery. This is most apparent in Grade II where the disc height is greatest (~ 11.4 mm) and the lowest glucose and oxygen concentrations are observed at the NP and inner AF (Figure 4A and Figure 6A). However, as the CEP transport route shortened with reduced disc height of Grade III (~ 8.8 mm) and Grade IV (~ 6.7 mm), the nutrient concentrations and pH within the NP increased. Focusing first on the total cell density model, this is evident in the contour plots (Figure 4A-6A) but is also

summarised in Figure 4C-6C where the centre-most value is compared for all degeneration grades. However, diffusion distance from the supply source is only one factor influencing the distribution of metabolites within the IVD. By considering the density of specifically metabolically active cells, rather than assuming that the total cell density present are contributing to consumption and production rates, the nutrient demands within the tissue are altered. Applying the active cell criteria resulted in an increase in glucose concentration (Figure 4A) and a reduction in lactic acid build-up due to glycolysis (Figure 5A). The greatest impact can be observed in the oxygen contour plots, Figure 6A, where there is a notable smoothening of the gradient through the AF due to the lowest activity within this domain and a significant increase in oxygen within the NP. To quantitatively compare total and active cell density, the predicted concentration profiles at mid-height through the IVD are presented in Figure 4B-6B. The predicted profiles are overlaid with values reported in the literature for the NP region of the disc. As previously highlighted in Figure 1, the overlaid glucose range is from published *in-silico* models[69–77], pH values are those experimentally measured together with a clinically relevant median value[65] and the oxygen range are experimental measurements which have been corrected for an elevated boundary concentration during the surgical procedure.[66]

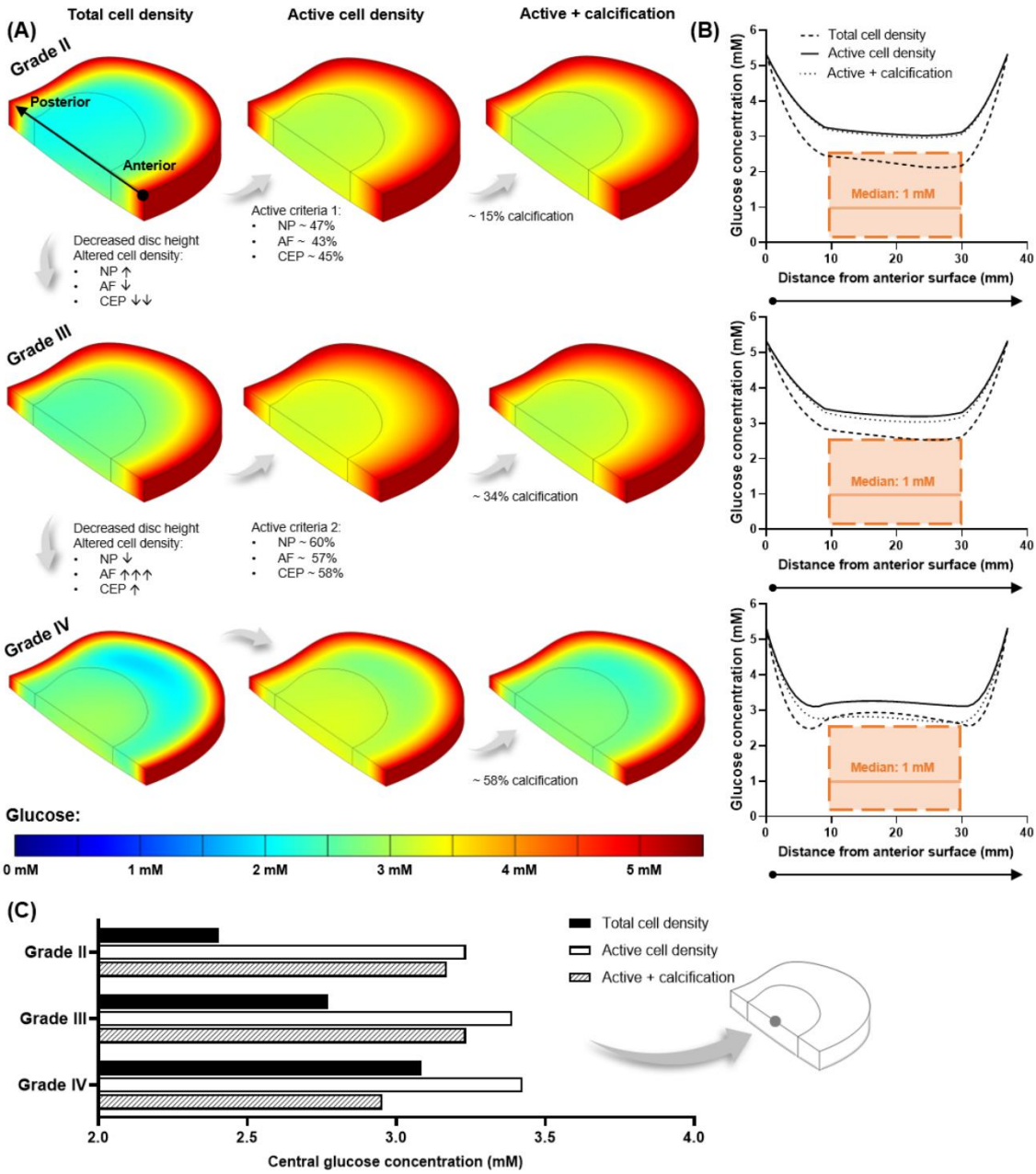

Figure 4. (A) Predicted glucose contour plots within a healthy adult (Grade II), mildly (Grade III) and moderately (Grade IV) degenerated *in-silico* intervertebral disc model. Each degeneration grade was investigated for a total cell density, a metabolically active cell density and the effect of cartilage endplate (CEP) calcification in the active model. Cell density was altered for degeneration grades, as highlighted for each tissue domain: ↑ and ↓ indicates < 30% increase and decrease, respectively; ↓↓ = ~ 60% decrease and ↑↑↑ = ~ 180% increase. (B) Predicted glucose profile at mid-height through the corresponding *in-silico* model, from the anterior to the posterior surface. The range of concentrations predicted within the nucleus pulposus (NP) by previously published models is overlaid in orange, together with a median value calculated across those studies. (C) Central glucose concentration for all three degeneration grades under each of the investigated conditions.

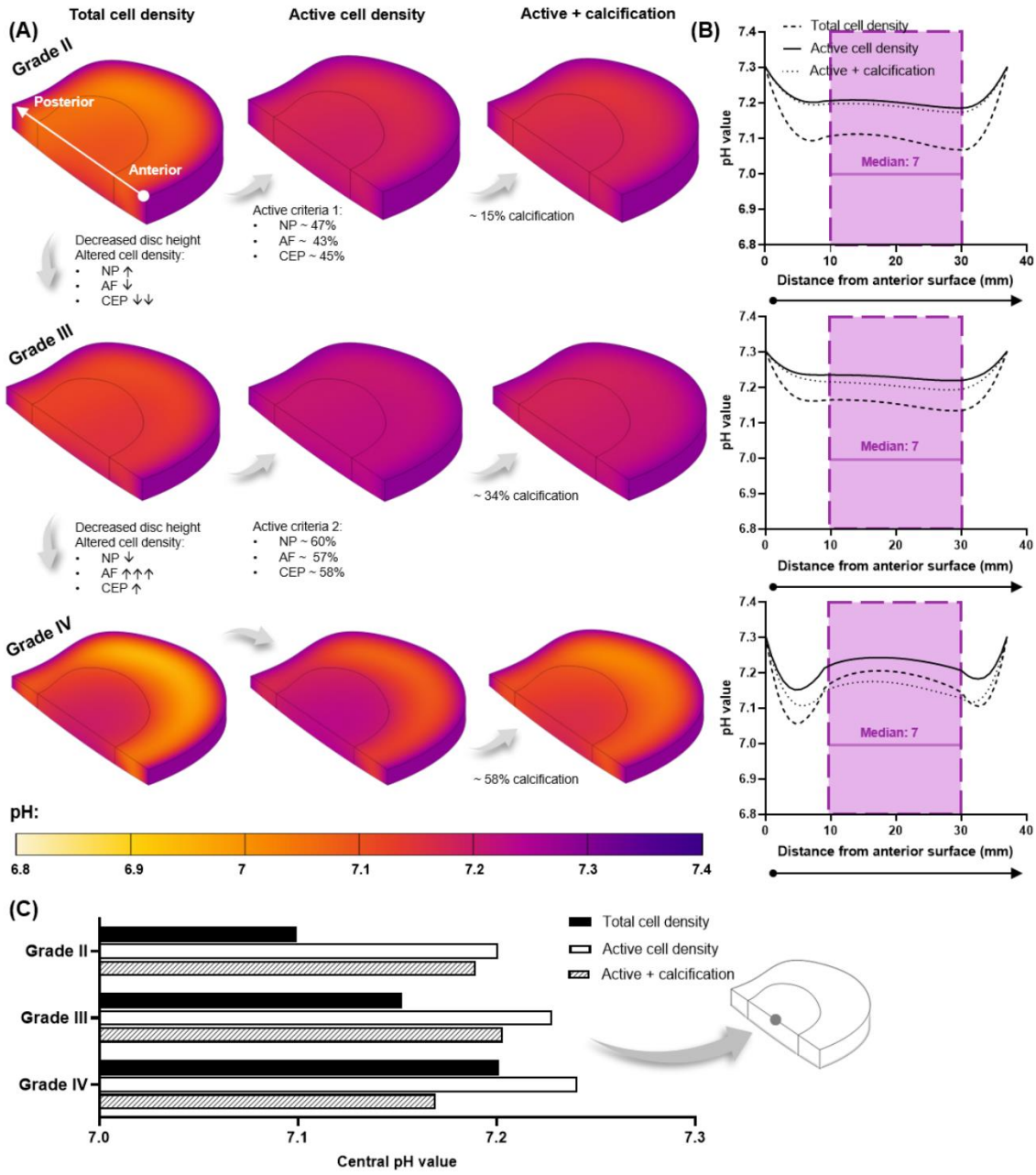

Figure 5. (A) Predicted pH contour plots within a healthy adult (Grade II), mildly (Grade III) and moderately (Grade IV) degenerated *in-silico* intervertebral disc model. Each degeneration grade was investigated for a total cell density, a metabolically active cell density and the effect of cartilage endplate (CEP) calcification in the active model. Cell density was altered for degeneration grades, as highlighted for each tissue domain: ↑ and ↓ indicates < 30% increase and decrease, respectively; ↓↓ = ~ 60% decrease and ↑↑↑ = ~ 180% increase. (B) Predicted pH profile at mid-height through the corresponding *in-silico* model, from the anterior to the posterior surface. The range of pH values measured with the nucleus pulposus (NP) is overlaid in purple, together with a clinically relevant median value.[65] (C) Central pH for all three degeneration grades under each of the investigated conditions.

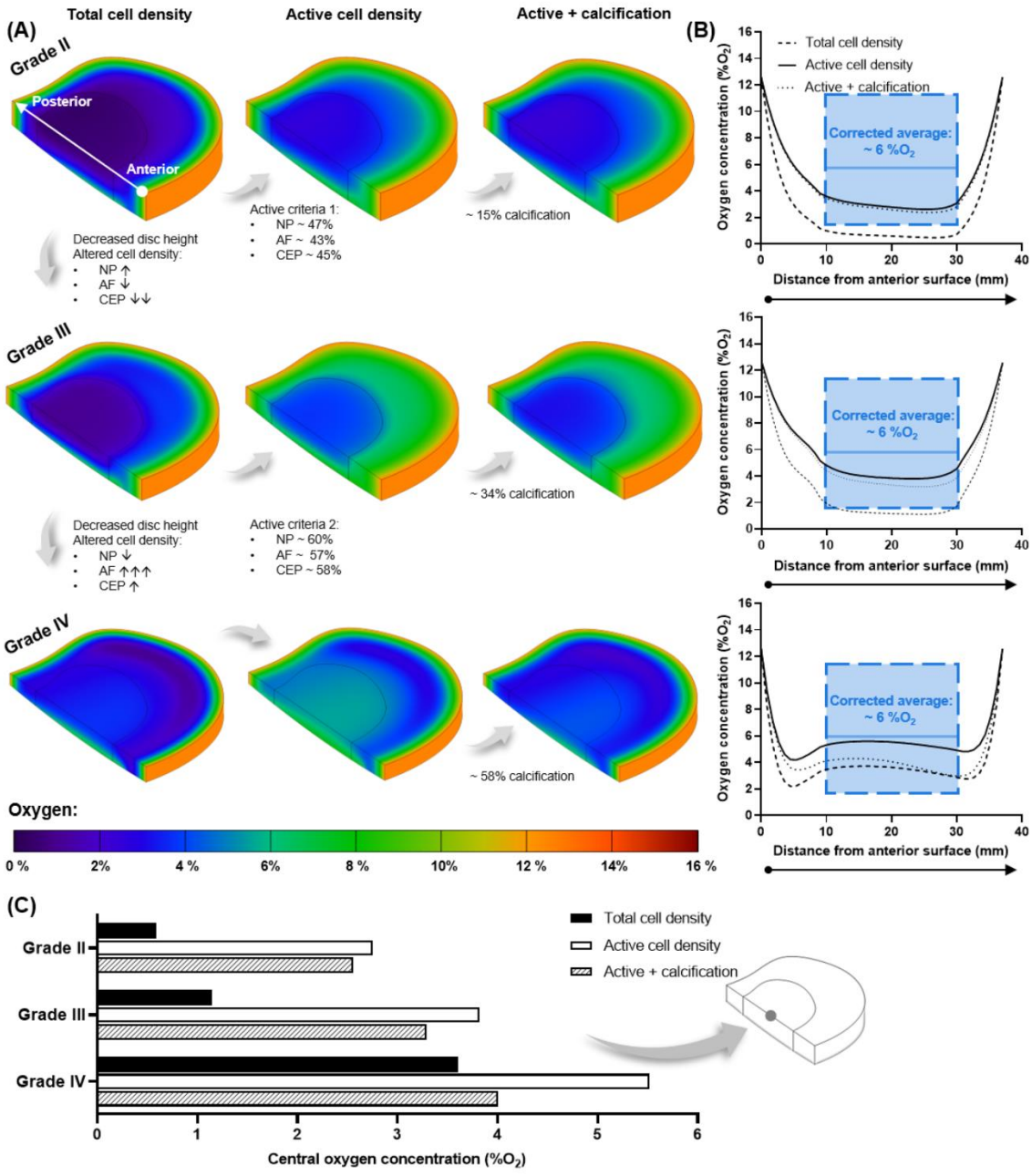

Figure 6. (A) Predicted oxygen contour plots within a healthy adult (Grade II), mildly (Grade III) and moderately (Grade IV) degenerated *in-silico* intervertebral disc model. Each degeneration grade was investigated for a total cell density, a metabolically active cell density and the effect of cartilage endplate (CEP) calcification in the active model. Cell density was altered for degeneration grades, as highlighted for each tissue domain: ↑ and ↓ indicates < 30% increase and decrease, respectively; ↓↓ = ~ 60% decrease and ↑↑↑ = ~ 180% increase. (B) Predicted oxygen profile at mid-height through each of the corresponding *in-silico* models, from the anterior surface to the posterior surface. The range of boundary corrected oxygen measurements within the nucleus pulposus (NP) and average central concentration are overlaid in blue.[66] (C) Predicted central oxygen concentration for all three degeneration grades under each of the investigated conditions.

While the number of metabolising cells influences the minimum concentrations within the IVD, changes in cell distribution between the NP, AF and CEP affect the metabolite gradients between degeneration grades. Focussing on the total and/or active cell density contour plots in Figure 4A-6A. When advancing from Grade II to mildly degenerated Grade III, not only does the axial transport route shorten but the CEP cell density decreases ~ 60%, facilitating greater diffusion of nutrients into the NP and metabolic waste out, despite modelling a slight increase in NP cell density (less than 30%). It is important to note this is assuming a constant boundary supply and not considering other impeding artefacts such as calcification at this point. Advancing from Grade III to moderately degenerated Grade IV, despite a slight increase in CEP cell density (less than 30%), further reduction in disc height and a slight decrease in NP cell density (less than 30%) predicts an increase in nutrient concentration in the NP. However, modelling a very significant increase in AF cell density (~ 180%) predicts greater impedance of nutrients through the peripheral AF transport route due to high consumption and a shift in the location of lowest nutrients laterally. Similarly, more concentrated lactate production within the densely populated degenerated AF results in greater acidity in the disc periphery rather than centrally. The effect of AF cell density in Grade IV is most apparent in the anterior and posterior regions of the metabolite profiles in Figure 4B-6B.

Calcification of the CEP, at each degeneration grade, decreased the glucose, pH and oxygen concentrations within the NP and inner AF, with close to no effect on the outer AF region. Calcification was simulated in the active cell density models only and the regional effects can be seen in both the contour plots (Figure 4A-6A) and the anterior to posterior profiles (Figure 4B-6B). At Grade II with ~ 15% calcification, a minor reduction on transport in and out of the NP through the CEP transport route was observed, with an insignificant effect on the central metabolite levels within the IVD (Figure 4C-6C). At Grade III (~ 34% calcification), nutrient concentrations did not appear to change significantly. Meanwhile Grade IV, with ~ 58%

calcification, resulted in nutrient and pH values dropping below those predicted within the NP for a total cell density (i.e., assuming every cell present is contributing to consumption). This can be seen in the anterior to posterior metabolite profiles for Grade IV (Figure 4B-6B) and in Figure 4C-6C where the centre-most glucose, pH and oxygen values are summarised for all degeneration grades under all investigated conditions.

Figure 7 (A-F) elucidates the effect of injecting 3, 6, 9 or 18 million into the NP of the calcified Grade III model. As expected, the concentration of nutrients and the pH reduces with an increase in the number of cells injected. As the cells are assumed to be homogenously injected into the NP, the change in metabolite concentrations within the disc are concentrated within the NP, as highlighted in the contour plots (A-C) and the A-P profile (D-F). Although the contour plots are not shown for Grade IV, the minimum nutrient concentrations and pH predicted within the NP for Grade III and IV are compared in Figure 7 (G-I).

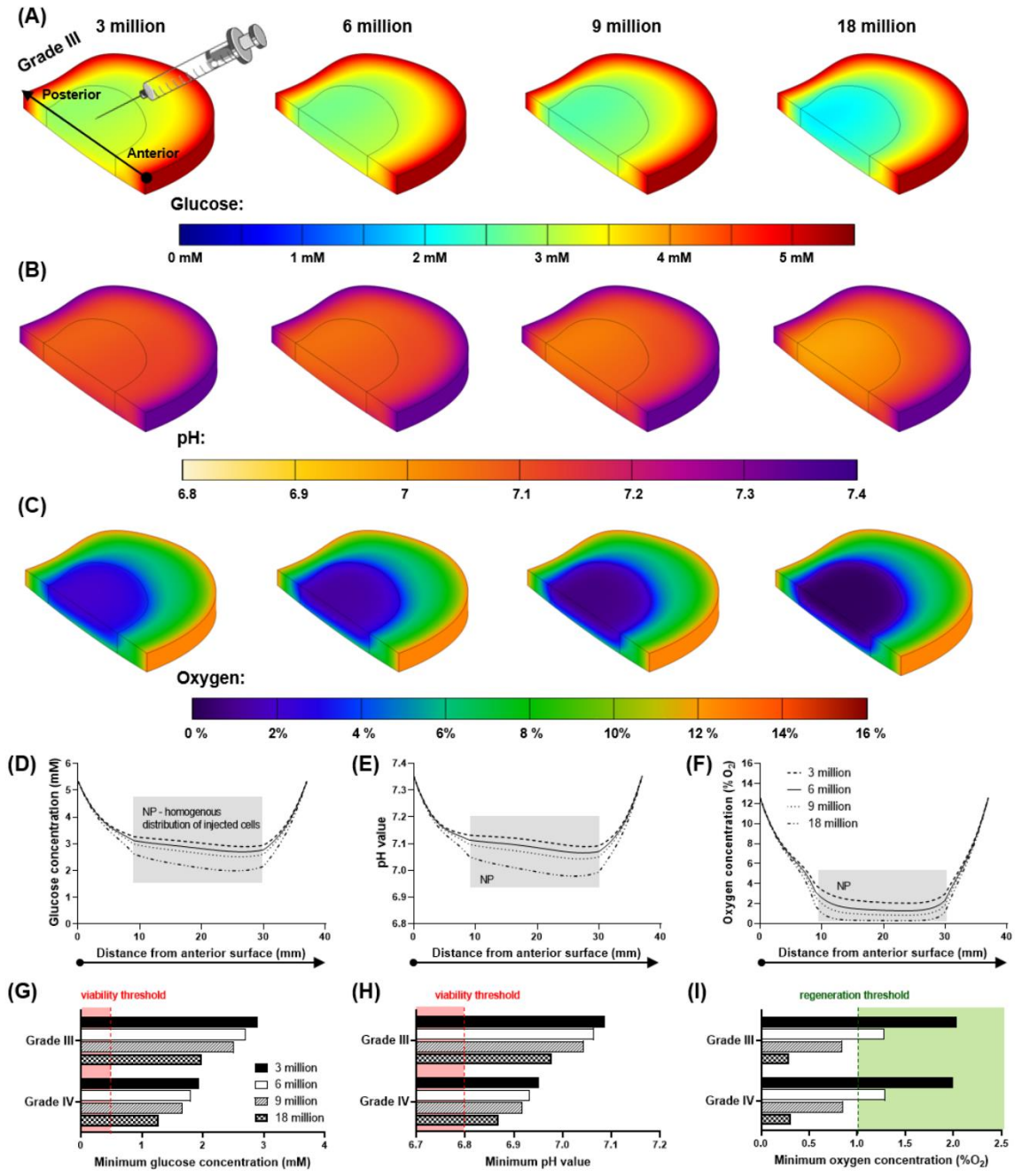

Figure 7. Predicted glucose (A), pH (B) and oxygen (C) contour plots for a calcified Grade III disc injected with 3, 6, 9 or 18 million discogenic cells. (D-F) Predicted metabolite profile at mid-height through each of the corresponding *in-silico* models, from the anterior surface to the posterior surface. The shaded region highlights the nucleus pulposus (NP) where the injected cells are assumed to be homogeneously distributed. The predicted minimum concentration of glucose (G), pH (H) and oxygen (I) within the NP of a calcified Grade III and Grade IV disc following transplantation of 3, 6, 9 or 18 million cells. The threshold below which cell viability is affected is highlighted in red for glucose and pH[38,39,113,115], while the oxygen concentration for optimal regeneration is highlighted in green.[42,116–119]

Discussion

Due to the avascularity of the IVD, tissue nutrient transport rates and inherent cell metabolic rates naturally give rise to concentration gradients. This work aimed to reflect on what is already known about these concentrations *in vivo* and re-evaluate them in terms of clinically relevant degeneration grades. Using *in-silico* modelling we incorporated newer experimental data on degeneration grade-specific metabolically active cell densities[90], tissue hydration[93,95–103], diffusion parameters[79–87] and calcification [89] and assessed the implications for developing cell-based regeneration strategies.

Disc cells primarily obtain their energy through anaerobic glycolysis making glucose the critical nutrient for disc cell survival.[14,42] However, there is a lack of directly measured values of glucose concentration in disc tissue and *in-silico* modelling is typically used to surmise or predict *in vivo* concentrations. Models presented in the literature have estimated a glucose range from 0.25 mM to above 2 mM with the median NP concentration across all the studies being 1 mM. Together these have established the conjecture that NP glucose concentrations are critically low, making it particularly inhospitable to potential cell therapies.[58,59,120] Although it is important to note that each of these studies investigated effects such as reducing nutrient supply or exchange area[69,75] and altering tissue diffusivity[69,71,72], particularly through reducing CEP permeability or porosity through parametric analysis.[73,74,77] Other osmo-mechanical properties include altering water content, fixed charge, deformation[70,74] and dynamic loading.[75,76] Despite significant advances interrelating metabolic rates[109,111] and incorporating cell death with nutrient deprivation[72,121], *in-silico* models remain limited by availability of experimental data, both as input parameters and for subsequent validation of predictions. Therefore, we believe that the multivariance models presented in this work advance the research field through pooled grade specific experimental data for more accurate modelling parameters of a dehydrated NP, anisotropic AF, and calcified CEP. Additionally, we

have consolidated what has previously been measured *in vivo* and used this information to help validate the predictive models with these key experimental studies.

We predicted slightly higher glucose concentrations within the disc compared with the overlaid range from previous reported *in-silico models* in the literature. As expected, the total cell density model was most comparable with the overlay, as the previous models had not accounted for a proportion of the cell population not being metabolically active. Overall, the current models predict a trend of increasing glucose concentration with degeneration (ignoring calcification in this instance), as there is a compensation of decreased diffusional distance due to reduced disc height. This has also been predicted in another *in-silico* model where halving the disc height reduced the cell death ratio through increasing critical glucose and reducing pH levels.[76] It is important to reiterate that the literature models investigate a wide range of parameters and several studies circumvent the lack of experimental input through parametric analysis.[69,71] Consequently, it is possible that the modelling scenarios presented for glucose are far more severe than the clinically relevant grades of degeneration being elucidated here, thus over-estimating the harshness of the microenvironment. Experimental glucose measurements in other species include dogs and pigs with one study reporting levels below 1 mM through micro-dialysis measurement, and the other measured a central NP concentration of ~ 3 mM through biochemical analysis.[61,122,123] Our predictive models are in good agreement with the latter and are more plausible in terms of sustaining the NP cell population which has been shown to experience significant cell death when glucose drops below 0.5 mM for more than 3 days.[38,39,109] Even with an array of predicted and measured glucose concentrations (0.25 – 3.5 mM) it is a relatively narrow range confined by the upper supply limit of blood glucose levels (2.6 – 6.1 mM).[32] Despite this more than 50% of publications utilising NP cells report high glucose culture medium (25 mM or 4.5 g/L). Together this highlights an urgency for robust experimental glucose measurements in healthy and degenerating human IVDs, not only to

permit validation of *in-silico* models but to significantly advance the field in fully elucidating the glucose microenvironment and refinement of *in vitro* culture conditions for physiological relevance.

A significant advancement in the current model is the availability of recent data on human cell densities and particularly metabolically active cell densities, which explains important differences with the *in-silico* literature. Previously, studies have relied on cell densities from early work, limited in sample size and donor age, while techniques have also developed and advanced significantly since.[82] The current work has greater precision at capturing degeneration grades by employing values from a study, with a far larger sample size, specifically investigating degeneration-related variation in cell density.[89] Furthermore, the inclusion of only cells positive for metabolic activity is particularly important as NP cells have been shown to experience a loss of both proliferative capacity and anabolic activity with normal aging and degeneration.[18,19] As captured by the results, when there is a reduction in the number of cells metabolising, there is an increase in the nutrient concentrations and a reduction in the build-up of lactic acid within the disc.

Additionally, the models capture a potential shift in the overall distribution of metabolites due to the changes in local cell density and activity between the different tissue domains. For example, pH was predicted to reduce within the AF of Grade IV, rather than the NP, due to an almost 2-fold increase in the total AF cell density and an increase in the percentage of active cells. However, the current model assumes no change in nutrient supply or waste removal, while the relationship between the surrounding microvasculature and transport is not straightforward. A recent review reported the prevalence of vascular ingrowths extending into the inner AF through degenerative fissures, which may explain the large increase in AF cell density and their ability to remain viable.[124,125] Alternatively, subchondral bone sclerosis and occlusion of marrow contact channels may affect the vertebral supply route, with a correlation

reported between functional capillary bud density and diffusion.[126,127] This may contribute to lower nutrient availability through the EP route[128–131], which could create a shift in the predominance of the transport routes. Thus, more quantitative measurements of nutrient supply and metabolite concentrations at the boundary of the IVD are needed to ascertain confidence in nutrient-transport models and may need to be assessed in a patient specific manner.

Acidity has been shown to be important for maintaining NP cell activity.[59] However, too low a pH is detrimental for proteoglycan (PG) synthesis rates which have been seen to reduce significantly below pH 6.8.[41,109,115] Hence, it is vital to consider the *in vivo* pH microenvironment at difference stages of degeneration in developing a cell therapy to survive and reach full regenerative capacity within the patient's specific microenvironment. Additionally, it is of utmost importance to re-evaluate the typical "disc-like" conditions used during *in vitro* cell assessment. As mentioned previously, a healthy state is typically represented by pH 7.1, mild degeneration by pH 6.8 and severe degeneration by pH 6.5.[22–26,30] However, when we visualise the data from Nachemson (1969) we see that the pH may not be as critically low as commonly believed (Figure 1 (C)). Only 4 out of 38 measurements were below 6.5 and each of these were noted as having an abundance of degenerative artifacts (granulation tissue, scars and adhesions) in conjunction with severe pain, thus making their degenerative state too advanced for regeneration through cell therapy.[10,57] A median value of pH 7 was observed across the three levels of back pain (excluding the aforementioned statistically different values). Furthermore, 50% of measurements were actually at or above pH 7 and only 18% of the + or ++ groups were below pH 7. Therefore, we believe that if cell-based therapies are to be used to suppress deterioration and restore IVD homeostasis, at an earlier stage of the degenerative cascade, then pH may not play as significant a role as commonly believed.

Human disc nutrient microenvironment

The pH profiles predicted in the current work all fall within the range of intradiscal measurements, although above the calculated median of pH 7. The total cell density model at Grade II and III, the most comparable to published literature as mentioned earlier, also show good agreement with *in-silico* models which predicted a range of 7 – 7.2 within the NP.[70,71,77] However, it is important to note that the intradiscal measurement range of 7 – 7.5 is large in terms of the pH scale and most prolapsed discs showed values above pH 7, although the author states that no statistical difference due to prolapse was demonstrable.[65] Our conjecture that pH may not be as critical as commonly believed is supported by human lactate concentrations of 2 – 6 mM (pH 7.3 – 6.9) from Bartels *et al.* (1998), which saw only one outlier below pH 6.5 in a disc adjacent to a fused motion segment.[66]

Oxygen plays a pivotal role in regulating the biosynthesis of native NP cells and many of the potential regenerative cell sources being explored.[117] Highest PG synthesis rates have been recorded at approximately 5 $\%O_2$ and synthesis appears to be inhibited significantly in an oxygen-dependent manner below this.[42] Although disc cells reside in an avascular niche which is commonly characterised as hypoxic, potential cell therapies are still often assessed under normoxic conditions (20 - 21 $\%O_2$).[22,24,28,29] "Physioxia" (~5 $\%O_2$) remains the most commonly accepted culturing condition *in vitro* for the musculoskeletal field. However, studies have used lower hypoxic concentrations of 0.1 - 1 $\%O_2$ and a higher concentration of 10 $\%O_2$.[27,29] Although lower oxygen appears to provide optimal functioning for native NP cells and some potential cell sources[59,132], hypoxia and matrix acidity are also linked to the progression of a pro-inflammatory microenvironment[133,134], in particular, interleukin-1 β (IL-1β) and tumour necrosis factor-α (TNF-α) which are believed to be critical in inducing degeneration of the ECM through cell senescence and upregulation of matrix metalloproteinases (MMPs).[135,136] Therefore, we need to consolidate what "physioxia" means in terms of the IVD microenvironment and re-evaluate the culturing conditions used *in vitro*.

The average lumbar profile curve fitted to the data of Bartels *et al.* (1998) suggests that the central NP concentration is slightly higher than traditional hypoxia (2 - 5 $\%O_2$), with a value of ~ 8 $\%O_2$ from the raw measurements or closer to 6 $\%O_2$ when corrected for the elevated oxygen administered during general anaesthesia (Supplementary Figure S1). In the current work, the oxygen profiles predicted for an active cell density fall within the range of intradiscal measurements, while the total cell density profiles fall just below the measured range. This supports our conviction that identifying the metabolically active cell density is a particularly important parameter for *in-silico* modelling. It is unlikely that in a healthy adult (Grade II) that NP cells could sustain ECM homeostasis at less than 1 $\%O_2$ as was predicted in the total cell density model. Like glucose, oxygen concentration appears to increase with degeneration and in particular, Grade IV shows good agreement with the overlayed measurements. This may be credible as the majority of patients undergoing spinal surgery were at least Grade IV.[66] Furthermore, a recent review also suggests that oxygen concentration increases with degeneration due to blood vessel invasion and speculates that this may in fact aggravate the "physioxic" conditions favoured by potential cell sources.[59] Therefore, the research field should re-evaluate the *in vivo* oxygen microenvironment in order to ascertain the clinical relevance of *in vitro* testing conditions and potentially consider patient or degeneration grade-specific treatments based on microenvironmental concentrations.

Like previous models, calcification effects were simulated in this work through reduced CEP diffusion[73], although degeneration grade specific levels of calcification were applied based on experimental quantification.[107] In this work, the levels of calcification at Grade II and Grade III were not predicted to significantly impact the central metabolite concentrations. Only at Grade IV did calcification appear to impede diffusion to a greater extent, with central glucose and pH levels dropping below those predicted of the total cell density models. Therefore, the current work suggests that at mild and moderate stages of degeneration, the effect of

calcification would not appear to be as critical a factor on nutrient supply as commonly speculated for cell-based regeneration, with the glucose concentration only reducing by less than 1 mM and oxygen concentration reducing by ~ 1.5 $\%O_2$ (Grade IV). However, if the central concentrations are lower than those predicted, then such a reduction in nutrients may be critical. Additionally, lactic acid build-up due to calcification did result in a 0.1 reduction on the pH scale. From this work we can only speculate that the effect of calcification becomes more pertinent at Grade V, which we have already deemed too degenerated for cell-based regeneration. It is also important to note that human disc histopathology studies have revealed that not all degenerated discs exhibit calcification of the CEPs.[137] Therefore, this work sought to capture models of each grade with and without calcification, despite the limitation of generic models of each grade with mean parameters rather than a range of plausible bounds to the mean.

When investigating the effect of injecting 3 – 18 million discogenic cells into the NP of a calcified Grade III and IV disc, the current work found that glucose and pH did not appear to be the limiting factor, with minimum concentrations remaining above the threshold at which viability has been reported to be impaired (0.5 mM glucose or pH 6.8).[38,39,113,115] However, simulating an injection of 9 or 18 million cells predicted that the oxygen level drops below 1 $\%O_2$. This is important in terms of the regenerative potential as studies have shown 5 $\%O_2$ oxygen to be optimal for GAG synthesis[42,117], while others have shown that hypoxia as low as 1 $\%O_2$ did not significantly reduce regenerative capacity.[116,118,119] Although the concentrations were not critical, comparing glucose and pH results for Grade III and IV show that it is likely that different cell numbers will be needed based on degeneration stage and patient-specific factors which affect the local microenvironment, as discussed previously. Interestingly, we did not see a difference in the minimum oxygen concentration between Grade III and IV due to the injected cells. This suggests that any reduction in disc height between grades compensates for

the effect of calcification, which is more prominent for the larger solutes (glucose and lactate). The current work, while considering all caveats of the in-silico models, suggests that 3 or 6 million cells is the optimal number for intradiscal injection. We believe that these results may provide further insight into the progression of clinical trials and the potential to refine the design of trials. For example, some of the earlier clinical trials used 20 – 60 million cells per disc[138–141], while more recent trials from Mesoblast Ltd. used 6 and 18 million cell doses in their Phase 2 trial (NCT01290367) before progressing into Phase 3 with just the lower dose of 6 million cells (NCT02412735). Additionally, DiscGenics Inc. used 10 million cells in their pre-clinical animal rabbit model[50], before progressing with a low dose of 3 million and a high dose of 6 million cells in their ongoing clinical trials (NCT03347708).

The causal link between degeneration and transport inadequacy remains complicated and a limitation of the current work is the assumption of pure diffusion, while mechanical loading could enhance nutrition through forced solute convection. This may be particularly important in aging and degeneration with the CEP becoming less porous, less hydrated and the presence of calcification impeding diffusion.[142] However, studies have also reported increased porosity, due to osteoporosis and osteochondral remodelling, and speculate it to be linked to degenerative features such as the loss of NP osmotic pressure, antigen exposure and immune inflammation.[143] Therefore, the significance of convection due to dynamic loading may vary significantly from patient to patient depending on individual matrix composition and porosity.

Conclusion

As tissue engineering and regenerative approaches advance rapidly there is a pressing need for a more thorough understanding of the metabolite concentrations present in the human IVD microenvironment and how they govern the behaviour of potential cell therapies. In this work we consolidated glucose, pH and oxygen levels previously measured or predicted within

the NP, with the aim of re-evaluating the microenvironment at stages of degeneration which are clinically relevant for cell-based regeneration. Additionally, we have advanced *in-silico* modelling through a strong foundation of experimentally determined grade-specific input parameters (diffusion coefficients, cell density, tissue hydration, disc height and CEP calcification). Taken together, pre-existing measurements and our predicted results suggest that metabolite concentrations may not be as critically low as commonly believed. In fact, nutrient concentrations may increase due to reduced disc height and vasculature ingrowth. Additionally, calcification does not appear to have a detrimental effect at earlier stages of degeneration when cell therapies are deemed an appropriate treatment. Ultimately the goal is to recapitulate the different microenvironmental niches *in vitro*, leading to more effective therapies with greater potential for reversing or slowing down degeneration in patient-specific microenvironments.

Acknowledgements

This work was supported by the Irish Research Council (IRC) - Government of Ireland Postgraduate Scholarship Scheme (GOIPG/2018/2448) and Science Foundation Ireland Career Development Award (15/CDA/3476).

Conflicts of Interest

The authors declare no conflicts of interest.

Authors' Contribution

Both authors contributed substantially to the conception and design of the work. Emily E. McDonnell performed the acquisition, analysis, and interpretation of literature data, computational modelling, analysis presentation and interpretation of results, drafting of the article, revising it critically and final approval. Conor T. Buckley, as the overall project funding holder, takes responsibility for the integrity of the work from inception to finalised article,

provided substantial contribution to data interpretation and presentation, drafting of the article, revising it critically, and final approval.

Supplementary Material

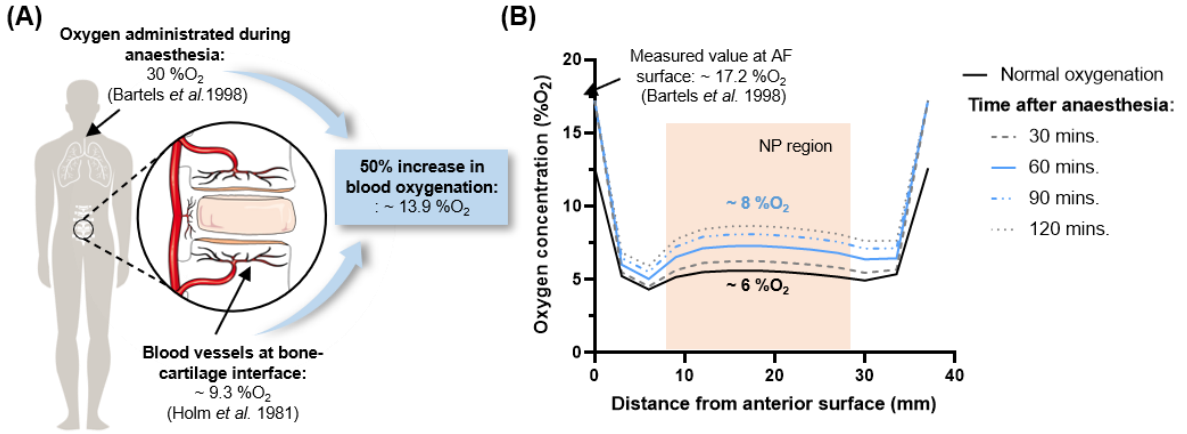

Supplementary Figure S1. (A) Bartels *et al.* (1998) reported that patients inhaled 30 $\%O_2$ for at least one hour as part of general anaesthesia, as a result oxygenation is increased by 50% compared to normal respired air. According to Holm & Selstam (1982) alterations in inspired oxygen would have caused an immediate change in arterial oxygen concentration (within 10 seconds) and an intradiscal response time of minutes (depending on the distance from the endplate). Taking all of this into consideration, an *in-silico* model was established with an elevated oxygen boundary condition at the bone-cartilage interface of the endplate. The oxygen concentration on the surface of the annulus fibrosus (AF) was measured by Bartels *et al.* (B) Firstly, the steady-state oxygen gradient through the disc is established for normal (basal) oxygenation levels (solid black line). Secondly, a time-dependent analysis was performed with elevated boundary concentrations to determine the effect of the duration of anaesthesia on the central oxygen concentrations. The profile at mid-height through the disc from the anterior to the posterior surface is presented graphically. Due to the elevated oxygen inhalation lasting at least 1 hour, we predict that the oxygen concentration is inflated by ~ 2 $\%O_2$ in the disc centre due to the cartilage endplate transport route.

Supplementary Table S2. Cell density parameters used in the nucleus pulposus (NP), annulus fibrosus (AF) and cartilage endplate (CEP) for each grade-specific *in-silico* model.

		Cell density (cells/mm^3)		
		NP	**AF**	**CEP**
Grade II	*Total*	2,452	2,432	27,215
	Active	1,155	1,048	12,246
Grade III	*Total*	3,183	1,855	10,149
	Active	1,499	800	4,567
Grade IV	*Total*	2,307	5,297	10,574
	Active	1,373	2,998	6,133

Supplementary Figure S3. (A) Model geometry for a quadrant of a L4/L5 intervertebral disc with distinct cartilage endplate (CEP), annulus fibrosus (AF) and nucleus pulposus (NP) regions. The lateral and anterior to posterior (A-P) widths remain constant with degeneration for each region and so does the thickness of the CEP. (B) The disc height reduces as a function of degeneration. Half the thickness of the disc is shown for the external edges and at the AF-NP interface for each grade. Additionally, the maximum central disc height has been added for the full thickness of the IVD.

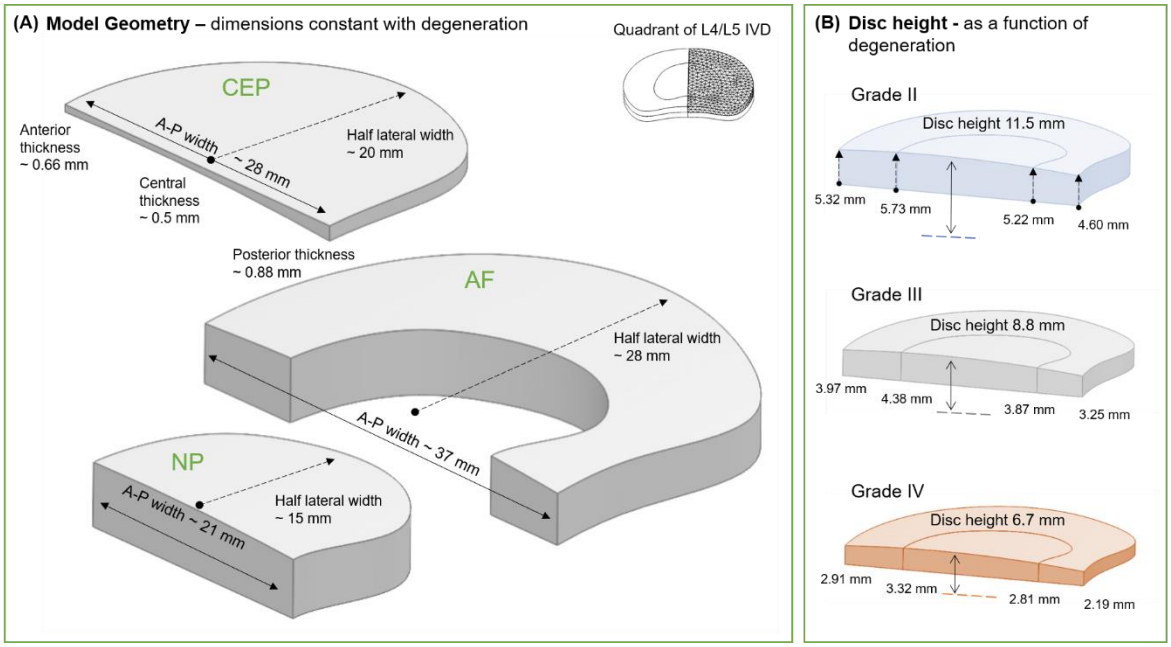

Supplementary Table S4. Finalised input parameters used in the grade-specific *in-silico* model to capture the effective diffusion of the relevant metabolites (oxygen, glucose, and lactate) through the nucleus pulposus (NP), annulus fibrosus (AF) and cartilage endplate (CEP).

		Diffusion coefficients (mm^2/hr)				
			AF		**CEP**	
		NP	*Axial*	*Radial*	*No calcification*	*Calcification*
Grade II	*Oxygen*	3.08	2.20	3.08	4.15	3.53
	Glucose	0.45	0.37	0.45	0.14	0.12
	Lactate	0.61	0.50	0.61	0.25	0.21
Grade III	*Oxygen*	3.08	2.20	3.08	4.15	2.74
	Glucose	0.45	0.37	0.45	0.14	0.09
	Lactate	0.61	0.50	0.61	0.25	0.16
Grade IV	*Oxygen*	3.08	2.20	3.08	4.15	1.74
	Glucose	0.45	0.37	0.45	0.14	0.06
	Lactate	0.61	0.50	0.61	0.25	0.10

References

1. Institute for Health Metrics and Evaluation (IHME). Global Burden of Disease Study 2017. *Lancet*. 2017;5:1-27. www.healthdata.org. Accessed July 8, 2021.
2. Foster NE, Anema JR, Cherkin D, et al. Prevention and treatment of low back pain: evidence, challenges, and promising directions. *Lancet*. 2018;391(10137):2368-2383. doi:10.1016/S0140-6736(18)30489-6
3. Hartvigsen J, Hancock MJ, Kongsted A, et al. What low back pain is and why we need to pay attention. *Lancet*. 2018;391(10137):2356-2367. doi:10.1016/S0140-6736(18)30480-X
4. Sivan SS, Wachtel E, Roughley PJ. Structure, function, aging and turnover of aggrecan in the intervertebral disc. *Biochim Biophys Acta - Gen Subj*. 2014;1840(10):3181-3189. doi:10.1016/j.bbagen.2014.07.013
5. Ohnishi T, Novais EJ, Risbud M V. Alterations in ECM signature underscore multiple sub- phenotypes of intervertebral disc degeneration. *Matrix Biol Plus*. 2020;(xxxx):100036. doi:10.1016/j.mbplus.2020.100036
6. Smith LJ, Nerurkar NL, Choi K-S, Harfe BD, Elliott DM. Degeneration and regeneration of the intervertebral disc: lessons from development. *Dis Model Mech*. 2011;4(1):31-41;
7. Tendulkar G, Chen T, Ehnert S, Kaps HP, Nüssler AK. Intervertebral disc nucleus repair: Hype or hope? *Int J Mol Sci*. 2019;20(15). doi:10.3390/ijms20153622
8. Binch ALA, Fitzgerald JC, Growney EA, Barry F. Cell-based strategies for IVD repair: clinical progress and translational obstacles. *Nat Rev Rheumatol*. 2021. doi:10.1038/s41584-020-00568-w
9. Sakai D, Andersson GBJ. Stem cell therapy for intervertebral disc regeneration: Obstacles and solutions. *Nat Rev Rheumatol*. 2015;11(4):243-256.

doi:10.1038/nrrheum.2015.13

10. Smith LJ, Silverman LI, Sakai D, et al. Advancing cell therapies for intervertebral disc regeneration from the lab to the clinic: Recommendations of the ORS spine section. *JOR Spine*. 2018;(July):e1036. doi:10.1002/jsp2.1036
11. Farhang N, Silverman LI, Bowles RD. Improving Cell Therapy Survival and Anabolism in Harsh Musculoskeletal Disease Environments. *Tissue Eng - Part B Rev*. 2020;26(4):348-366. doi:10.1089/ten.teb.2019.0324
12. Boos N, Weissbach S, Rohrbach H, Weiler C, Spratt KF, Nerlich AG. Classification of age-related changes in lumbar intervertebral discs: 2002 Volvo award in basic science. *Spine (Phila Pa 1976)*. 2002;27(23):2631-2644;
13. Nachemson A, Lewin T, Maroudas A, Freeman MAR. In vitro diffusion of dye through the end-plates and the annulus fibrosus of human lumbar inter-vertebral discs. *Acta Orthop*. 1970;41(6):589-607. doi:10.3109/17453677008991550
14. Holm S, Maroudas A, Urban JPG, Selstam G, Nachemson A. Nutrition of the Intervertebral Disc: Solute Transport and Metabolism. *Connect Tissue Res*. 1981;8(2):101-119;
15. Urban JPG, Holm S. Nutrition of the intervertebral disc: effect of fluid flow on solute transport. *Clin Orthop Relat Res*. 1982;(170):296-302;
16. Urban JPG, Maroudas A. The measurement of fixed charged density in the intervertebral disc. *Biochim Biophys Acta - Gen Subj*. 1979;586(1):166-178. doi:10.1016/0304-4165(79)90415-X
17. Grunhagen T, Shirazi-Adl A, Fairbank JCT, Urban JPG. Intervertebral Disk Nutrition: A Review of Factors Influencing Concentrations of Nutrients and Metabolites. *Orthop Clin North Am*. 2011;42(4):465-477. doi:10.1016/j.ocl.2011.07.010
18. Richardson SM, Knowles R, Tyler J, Mobasheri A, Hoyland JA. Expression of glucose

transporters GLUT-1, GLUT-3, GLUT-9 and HIF-1α in normal and degenerate human intervertebral disc. *Histochem Cell Biol*. 2008;129(4):503-511. doi:10.1007/s00418-007-0372-9

19. Agrawal A, Guttapalli A, Narayan S, Albert TJ, Shapiro IM, Risbud M V. Normoxic stabilization of HIF-1α drives glycolytic metabolism and regulates aggrecan gene expression in nucleus pulposus cells of the rat intervertebral disk. *Am J Physiol - Cell Physiol*. 2007;293(2):621-631. doi:10.1152/ajpcell.00538.2006
20. Wang F, Shi R, Wang Y-T, Wu X-T. Stem cell approaches to intervertebral disc regeneration: obstacles from the disc microenvironment. *Stem Cells Dev*. 2015;24(21):2479-2495.
21. Uchiyama Y, Cheng CC, Danielson KG, et al. Expression of Acid-Sensing Ion Channel 3 (ASIC3) in nucleus pulposus cells of the intervertebral disc is regulated by p75NTR and ERK signaling. *J Bone Miner Res*. 2007;22(12):1996-2006. doi:10.1359/jbmr.070805
22. Naqvi SM, Buckley CT. Differential response of encapsulated nucleus pulposus and bone marrow stem cells in isolation and coculture in alginate and chitosan hydrogels. *Tissue Eng - Part A*. 2015;21(1-2):288-299. doi:10.1089/ten.tea.2013.0719
23. Wuertz K, Godburn K, Iatridis JC. MSC response to pH levels found in degenerating intervertebral discs. *Biochem Biophys Res Commun*. 2009;379(4):824-829. doi:10.1016/j.bbrc.2008.12.145
24. Naqvi SM, Buckley CT. Bone marrow stem cells in response to intervertebral disc-like matrix acidity and oxygen concentration implications for cell-based regenerative therapy. *Spine (Phila Pa 1976)*. 2016;41(9):743-750. doi:10.1097/BRS.0000000000001314
25. Wuertz K, Godburn K, Neidlinger-Wilke C, Urban J, Iatridis JC. Behavior of

mesenchymal stem cells in the chemical microenvironment of the intervertebral disc. *Spine (Phila Pa 1976)*. 2008;33(17):1843-1849. doi:10.1097/BRS.0b013e31817b8f53

26. Li H, Liang C, Tao Y, et al. Acidic pH conditions mimicking degenerative intervertebral discs impair the survival and biological behavior of human adipose-derived mesenchymal stem cells. *Exp Biol Med*. 2012;237(7):845-852. doi:10.1258/ebm.2012.012009
27. Grimshaw MJ, Mason RM. Bovine articular chondrocyte function in vitro depends upon oxygen tension. *Osteoarthr Cartil*. 2000;8(5):386-392. doi:10.1053/joca.1999.0314
28. Scotti C, Osmokrovic A, Wolf F, et al. Response of human engineered cartilage based on articular or nasal chondrocytes to interleukin-1β and low oxygen. *Tissue Eng - Part A*. 2012;18(3-4):362-372. doi:10.1089/ten.tea.2011.0234
29. Malda J, Rouwkema J, Martins D, et al. Oxygen Gradients in Tissue-Engineered PEGT/PBT Cartilaginous Constructs: Measurement and Modeling. *Biotechnol Bioeng*. 2004;86(1):9-18;
30. Borrelli CM, Buckley CT. Synergistic effects of acidic ph and pro-inflammatory cytokines il-1β and tnf-α for cell-based intervertebral disc regeneration. *Appl Sci*. 2020;10(24):1-17. doi:10.3390/app10249009
31. Keeley TP, Mann GE. Defining physiological normoxia for improved translation of cell physiology to animal models and humans. *Physiol Rev*. 2019;99(1):161-234. doi:10.1152/physrev.00041.2017
32. Wang Y, Xu W, Zhang Q, et al. Follow-up of blood glucose distribution characteristics in a health examination population in Chengdu from 2010 to 2016. *Med (United States)*. 2018;97(8). doi:10.1097/MD.0000000000009763
33. Roberts S, Menage J, Eisenstein SM. The cartilage end-plate and intervertebral disc in scoliosis: Calcification and other sequelae. *J Orthop Res*. 1993;11(5):747-757;

34. Bernick S, Cailliet R. Vertebral end-plate changes with aging of human vertebrae. *Spine (Phila Pa 1976)*. 1982;7(2):97-102. doi:10.1097/00007632-198203000-00002

35. Roberts S, Urban JPG, Evans H, Eisenstein SM. Transport Properties of the Human Cartilage Endplate in Relation to Its Composition and Calcification. *Spine (Phila Pa 1976)*. 1996;21(4):415-420.

36. Grant MP, Epure LM, Bokhari R, Roughley PJ, Antoniou J, Mwale F. Human cartilaginous endplate degeneration is induced by calcium and the extracellular calcium-sensing receptor in the intervertebral disc. *Eur Cells Mater*. 2016;32(514):137-151. doi:10.22203/eCM.v032a09

37. Fields AJ, Ballatori A, Liebenberg EC, Lotz JC. Contribution of the Endplates to Disc Degeneration. *Curr Mol Biol Reports*. 2018;4(4):151-160. doi:10.1007/s40610-018-0105-y

38. Horner HA, Urban JPG. 2001 Volvo Award Winner in Basic Science Studies: Effect of nutrient supply on the viability of cells from the nucleus pulposus of the intervertebral disc. *Spine (Phila Pa 1976)*. 2001;26(23):2543-2549;

39. Bibby S, Urban JPG. Effect of nutrient deprivation on the viability of intervertebral disc cells. *Eur Spine J*. 2004;13(8):695-701;

40. Oshima H, Ishihara H, Urban JPG, Tsuji H. The use of coccygeal discs to study intervertebral disc metabolism. *J Orthop Res*. 1993;11(3):332-338;

41. Ohshima H, Urban JPG. The effect of lactate and ph on proteoglycan and protein synthesis rates in the intervertebral disc. *Spine (Phila Pa 1976)*. 1992;17(9):1079-1082. doi:10.1097/00007632-199209000-00012

42. Ishihara H, Urban JPG. Effects of low oxygen concentrations and metabolic inhibitors on proteoglycan and protein synthesis rates in the intervertebral disc. *J Othopaedic Res*. 1999;17(6):829-835;

43. Wong J, Sampson SL, Bell-Briones H, et al. Nutrient supply and nucleus pulposus cell function: effects of the transport properties of the cartilage endplate and potential implications for intradiscal biologic therapy. *Osteoarthr Cartil*. 2019;27(6):956-964. doi:10.1016/j.joca.2019.01.013

44. Dolor A, Sampson SL, Lazar AA, Lotz JC, Szoka FC, Fields AJ. Matrix modification for enhancing the transport properties of the human cartilage endplate to improve disc nutrition. *PLoS One*. 2019;14(4):1-18. doi:10.1371/journal.pone.0215218

45. Peck SH, Bendigo JR, Tobias JW, et al. Hypoxic Preconditioning Enhances Bone Marrow–Derived Mesenchymal Stem Cell Survival in a Low Oxygen and Nutrient-Limited 3D Microenvironment. *Cartilage*. 2019. doi:10.1177/1947603519841675

46. Naqvi SM, Gansau J, Gibbons D, Buckley CT. In Vitro Co-culture and Ex Vivo Organ Culture Assessment of Primed and Cryopreservation Stromal Cell. *Eur Cells Mater*. 2019;37:134-152.

47. Gansau J, Buckley CT. Priming as a strategy to overcome detrimental PH effects on cells for intervertebral disc regeneration. *Eur Cells Mater*. 2021. doi:10.22203/eCM.v041a11

48. Chiang ER, Ma HL, Wang JP, et al. Use of Allogeneic Hypoxic Mesenchymal Stem Cells For Treating Disc Degeneration in Rabbits. *J Orthop Res*. 2019;37(6):1440-1450. doi:10.1002/jor.24342

49. Wang W, Wang Y, Deng G, et al. Transplantation of hypoxic-preconditioned bone mesenchymal stem cells retards intervertebral disc degeneration via enhancing implanted cell survival and migration in rats. *Stem Cells Int*. 2018;2018. doi:10.1155/2018/7564159

50. Silverman LI, Dulatova G, Tandeski T, et al. In Vitro and In Vivo Evaluation of Discogenic Cells, An Investigational Cell Therapy for Disc Degeneration. *Spine J*. 2019.

doi:10.1016/j.spinee.2019.08.006

51. Hiraishi S, Schol J, Sakai D, et al. Discogenic cell transplantation directly from a cryopreserved state in an induced intervertebral disc degeneration canine model. *JOR Spine*. 2018;1(2):e1013. doi:10.1002/jsp2.1013
52. Borrelli CM, Buckley CT. Injectable Disc-Derived ECM Hydrogel Functionalised with Chondroitin Sulfate for Intervertebral Disc Regeneration. *Acta Biomater*. 2020. doi:10.1016/j.actbio.2020.10.002
53. Peng Y, Qing X, Lin H, et al. Decellularized Disc Hydrogels for hBMSCs tissue-specific differentiation and tissue regeneration. *Bioact Mater*. 2021;6(10):3541-3556. doi:10.1016/j.bioactmat.2021.03.014
54. Schol J, Sakai D. Cell therapy for intervertebral disc herniation and degenerative disc disease: clinical trials. *Int Orthop*. 2019;43(4):1011-1025. doi:10.1007/s00264-018-4223-1
55. Meisel HJ, Agarwal N, Hsieh PC, et al. Cell Therapy for Treatment of Intervertebral Disc Degeneration: A Systematic Review. *Glob Spine J*. 2019;9(1_suppl):39S-52S. doi:10.1177/2192568219829024
56. Vadalà G, Ambrosio L, Russo F, Papalia R, Denaro V. Stem Cells and Intervertebral Disc Regeneration Overview –– What They Can and Can ' t Do Stem Cells and Intervertebral Disc Regeneration Overview — What They Can and Can ' t Do. 2021;(April). doi:10.14444/8054
57. Buckley CT, Hoyland JA, Fujii K, Pandit A, Iatridis JC, Grad S. Critical aspects and challenges for intervertebral disc repair and regeneration-Harnessing advances in tissue engineering. *JOR Spine*. 2018;(July):e1029. doi:10.1002/jsp2.1029
58. Vadalà G, Ambrosio L, Russo F, Papalia R. Interaction between Mesenchymal Stem Cells and Intervertebral Disc Microenvironment : From Cell Therapy to Tissue

Engineering. *Stem Cells Int*. 2019.

59. Guerrero J, Häckel S, Croft A, Hoppe S, Albers C, Gantenbein B. The nucleus pulposus microenvironment in the intervertebral disc: the fountain of youth? *Eur Cells Mater*. 2021;41:707-738. doi:10.22203/ecm.v041a46

60. Ju DG, Kanim LE, Bae HW. Is There Clinical Improvement Associated With Intradiscal Therapies? A Comparison Across Randomized Controlled Studies. *Glob Spine J*. 2020. doi:10.1177/2192568220963058

61. Holm S, Selstam G, Nachemson A. Carbohydrate metabolism and concentration profiles of solutes in the canine lumbar intervertebral disc. *Acta Physiol Scand*. 1982;115(1):147-156;

62. Holm S, Nachemson A. Nutritional changes in the canine intervertebral disc after spinal fusion. *Clin Orthop Relat Res*. 1982;169:243-258. http://www.embase.com/search/results?subaction=viewrecord&from=export&id=L12021038.

63. Holm S, Selstam G. Oxygen tension alterations in the intervertebral disc as a response to changes in the arterial blood. *Ups J Med Sci*. 1982;87(2):163-174. doi:10.3109/03009738209178421

64. Kobayashi S, Baba H, Takeno K, Miyazaki T, Meir A, Urban JPG. Physical Limitations to Tissue Engineering of Intervertabral Disc Cells. *Tissue Eng*. 2010:247-281.

65. Nachemson A. Intradiscal measurements of ph in patients with lumbar rhizopathies. *Acta Orthop*. 1969;40(1):23-42. doi:10.3109/17453676908989482

66. Bartels EM, Fairbank JCT, Winlove PC, Urban JPG. Oxygen and lactate concentrations measured in vivo in the intervertebral discs of patients with scoliosis and back pain. *Spine (Phila Pa 1976)*. 1998;23(1):1-8;

67. Bibby S, Fairbank JCT, Urban MR, Urban JPG. Cell viability in scoliotic discs in

relation to disc deformity and nutrient levels. *Spine (Phila Pa 1976)*. 2002;27(20):2220-2228;

68. Schmidt H, Galbusera F, Rohlmann A, Shirazi-Adl A. What have we learned from finite element model studies of lumbar intervertebral discs in the past four decades? *J Biomech*. 2013;46(14):2342-2355;
69. Sélard E, Shirazi-Adl A, Urban JPG. Finite element study of nutrient diffusion in the human intervertebral disc. *Spine (Phila Pa 1976)*. 2003;28(17):1945-1953;
70. Magnier C, Boiron O, Wendling-Mansuy S, Chabrand P, Deplano V. Nutrient distribution and metabolism in the intervertebral disc in the unloaded state: A parametric study. *J Biomech*. 2009;42(2):100-108;
71. Soukane DM, Shirazi-Adl A, Urban JPG. Investigation of solute concentrations in a 3D model of intervertebral disc. *Eur Spine J*. 2009;18(2):254-262;
72. Shirazi-Adl A, Taheri M, Urban JPG. Analysis of cell viability in intervertebral disc: Effect of endplate permeability on cell population. *J Biomech*. 2010;43(7):1330-1336;
73. Jackson AR, Huang C-YC, Gu WY. Effect of endplate calcification and mechanical deformation on the distribution of glucose in intervertebral disc: a 3D finite element study. *Comput Methods Biomech Biomed Engin*. 2011;14(2):195-204;
74. Jackson AR, Huang C-YC, Brown MD, Gu WY. 3D Finite Element Analysis of Nutrient Distributions and Cell Viability in the Intervertebral Disc: Effects of Deformation and Degeneration. *J Biomech Eng*. 2011;133(9). doi:10.1115/1.4004944
75. Zhu Q, Jackson AR, Gu WY. Cell viability in intervertebral disc under various nutritional and dynamic loading conditions: 3d Finite element analysis. *J Biomech*. 2012;45(16):2769-2777;
76. Galbusera F, Mietsch A, Schmidt H, Wilke HJ, Neidlinger-Wilke C. Effect of intervertebral disc degeneration on disc cell viability: a numerical investigation. *Comput*

Methods Biomech Biomed Engin. 2013;16(3):328-337;

77. Wu Y, Cisewski SE, Sachs BL, Yao H. Effect of cartilage endplate on cell based disc regeneration: a finite element analysis. *Mol Cell Biomech*. 2015;10(2):159-182;
78. Diamant B, Karlsson J, Nachemson A. Correlation between lactate levels and pH in discs of patients with lumbar rhizopathies. *Experientia*. 1968;24(12):1195-1196. doi:10.1007/BF02146615
79. Boubriak OA, Lee RB, Urban JPG. Nutrient supply to cells of the intervertebral disc; effect of diurnal hydration changes. In: *49th Annual Meeting of the Orthopaedic Research Society*. Vol Poster #11. ; 2003:1127.
80. Jackson AR, Yuan T-Y, Huang C-YC, Travascio F, Gu WY. Effect of Compression and Anisotropy on the Diffusion of Glucose in Annulus Fibrosus. *Spine (Phila Pa 1976)*. 2008;33(1):1-7;
81. Jackson AR, Yuan T-Y, Huang C-YC. Nutrient Transport in Human Annulus Fibrosus is Affected by Compressive Strain and Anisotropy. *Ann Biomed Eng*. 2012;40(12):1-8;
82. Maroudas A, Stockwell R, Nachemson A, Urban JPG. Factors involved in the nutrition of the human lumbar intervertebral disc: cellularity and diffusion of glucose in vitro. *J Anat*. 1975;120(1):113-130;
83. Wu Y, Cisewski SE, Wegner N, et al. Region and strain-dependent diffusivities of glucose and lactate in healthy human cartilage endplate. *J Biomech*. 2016;49(13):2756-2762. doi:10.1016/j.jbiomech.2016.06.008
84. Yuan T-Y, Jackson AR, Huang C-YC, Gu WY. Strain-Dependent Oxygen Diffusivity in Bovine Annulus Fibrosus. *J Biomech Eng*. 2009;131:074503. doi:10.1115/1.3127254
85. Haselgrove JC, Shapiro IM, Silverton SF. Computer modeling of the oxygen supply and demand of cells of the avian growth cartilage. *Am J Physiol - Cell Physiol*. 1993. doi:10.1152/ajpcell.1993.265.2.c497

86. Burstein D, Gray ML, Hartman AL, Gipe R, Foy BD. Diffusion of small solutes in cartilage as measured by nuclear magnetic resonance (NMR) spectroscopy and imaging. *J Orthop Res*. 1993;11(4):465-478. doi:10.1002/jor.1100110402

87. Obradovic B, Meldon JH, Freed LE, Vunjak-Novakovic G. Glycosaminoglycan deposition in engineered cartilage: Experiments and mathemetical model. *AIChE J*. 2000. doi:10.1002/aic.690460914

88. Wu Y, Cisewski SE, Sachs BL, et al. The region-dependent biomechanical and biochemical properties of bovine cartilaginous endplate. *J Biomech*. 2015;48(12):3185-3191. doi:10.1016/j.jbiomech.2015.07.005

89. Liebscher T, Haefeli M, Wuertz K, Nerlich AG, Boos N. Age-Related Variation in Cell Density of Human Lumbar Intervertebral Disc. *Spine (Phila Pa 1976)*. 2011;36(2):153-159;

90. Martins D, Medeiros VP De, Wajchenberg M, et al. Changes in human intervertebral disc biochemical composition and bony end plates between middle and old age. *PLoS One*. 2018;13(9):1-17. doi:10.1371/journal.pone.0203932

91. O'Connell GD, Vresilovic EJ, Elliott DM. Comparison of Animals Used in Disc Research to Human Lumbar Disc Geometry. *Spine (Phila Pa 1976)*. 2007;32(3):328-333;

92. Galbusera F, Van Rijsbergen M, Ito K. Ageing and degenerative changes of the intervertebral disc and their impact on spinal flexibility. *Eur Spine J*. 2014;23(SUPPL. 3).

93. Delucca JF, Peloquin JM, Smith LJ, Wright AC, Vresilovic EJ, Elliott DM. MRI Quantification of Human Spine Cartilage Endplate Geometry : Comparison With Age , Degeneration , Level , and Disc Geometry. *J Orthop Res*. 2016;(August):1410-1417. doi:10.1002/jor.23315

94. Higgins J, Li T, Deeks JJ. Chapter 6: Choosing effect measures and computing estimates of effect. In: *Cochrane Handbook for Systematic Reviews of Interventions Version 6.2*. ; 2021.

95. Antoniou J, Steffen T, Nelson F, et al. The Human Lumbar Intervertebral Disc Evidence for Changes in the Biosynthesis and Denaturation of the Extracellular Matrix with Growth, Maturation, Ageing, and Degeneration. *J Clin Invest*. 1996;98(4):996-1003.

96. Iatridis JC, MacLean JJ, O'Brien M, Stokes IAF. Measurements of proteoglycan and water content distribution in human lumbar intervertebral discs. *Spine (Phila Pa 1976)*. 2007;32(14):1493-1497. doi:10.1097/BRS.0b013e318067dd3f

97. Showalter BL, Beckstein JC, Martin JT, et al. Comparison of animal discs used in disc research to human lumbar disc: Torsion mechanics and collagen content. *Spine (Phila Pa 1976)*. 2012;37(15). doi:10.1097/BRS.0b013e31824d911c

98. Lyons G, Eisenstein SM, Sweet MBE. Biochemical changes in intervertebral disc degeneration. *Biochim Biophys Acta*. 1981;673:443-453. doi:10.1016/0304-4165(81)90476-1

99. Gu WY, Mao XG, Foster RJ, Weidenbaum M, Mow VC, Rawlins BA. The anisotropic hydraulic permeability of human lumbar anulus fibrosus: Influence of age, degeneration, direction, and water content. *Spine (Phila Pa 1976)*. 1999;24(23):2449-2455. doi:10.1097/00007632-199912010-00005

100. Acaroglu ER, Iatridis JC, Setton LA, Foster RJ, Mow VC, Weidenbaum M. Degeneration and Aging Affect the Tensile Behavior of Human Lumbar Anulus Fibrosus. *Spine (Phila Pa 1976)*. 1995.

101. Antoniou J, Goudsouzian NM, Heathfield TF, et al. The human lumbar endplate. Evidence of changes in biosynthesis and denaturation of the extracellular matrix with growth, maturation, aging, and degeneration. *Spine (Phila Pa 1976)*. 1996;21(10):1153-

1161;

102. Bishop PB, Pearce RH. The proteoglycans of the cartilaginous end-plate of the human intervertebral disc change after maturity. *J Orthop Res*. 1993;11(3):324-331. doi:10.1002/jor.1100110303

103. Bishop PB. Changes in the proteoglycans of the intervertebral disc cartilaginous endplate with aging and degeneration. 1989;(July 1989).

104. Costi JJ, Stokes IA, Gardner-Morse M, Laible JP, Scoffone HM, Iatridis JC. Direct measurement of intervertebral disc maximum shear strain in six degrees of freedom: Motions that place disc tissue at risk of injury. *J Biomech*. 2007. doi:10.1016/j.jbiomech.2006.11.006

105. Heuer F, Schmidt H, Wilke HJ. The relation between intervertebral disc bulging and annular fiber associated strains for simple and complex loading. *J Biomech*. 2008. doi:10.1016/j.jbiomech.2007.11.019

106. O'Connell GD, Johannessen W, Vresilovic EJ, Elliott DM. Human internal disc strains in axial compression measured noninvasively using magnetic resonance imaging. *Spine (Phila Pa 1976)*. 2007. doi:10.1097/BRS.0b013e31815b75fb

107. Tomaszewski KA, Walocha JA, Mizia E, Gładysz T, Głowacki R, Tomaszewska R. Age- and degeneration-related variations in cell density and glycosaminoglycan content in the human cervical intervertebral disc and its endplates. *Polish J Pathol*. 2015;66(3):296-309. doi:10.5114/pjp.2015.54964

108. Soukane DM, Shirazi-Adl A, Urban JPG. Analysis of Nonlinear Coupled Diffusion of Oxygen and Lactic Acid in Intervertebral Discs. *J Biomech Eng*. 2005;127(12):1121-1126;

109. Bibby S, Jones D a, Ripley RM, Urban JPG. Metabolism of the intervertebral disc: effects of low levels of oxygen, glucose, and pH on rates of energy metabolism of bovine

nucleus pulposus cells. *Spine (Phila Pa 1976)*. 2005;30(5):487-496;

110. Huang C-YC, Yuan T-Y, Jackson AR, Hazbun L, Fraker C, Gu WY. Effects of Low Glucose Concentrations on Oxygen Consumption Rates of Intervertebral Disc Cells. *Spine (Phila Pa 1976)*. 2007;32(19):2063-2069;
111. Huang C-YC, Gu WY. Effects of mechanical compression on metabolism and distribution of oxygen and lactate in intervertebral disc. *J Biomech*. 2008;41(6):1184-1196;
112. McDonnell EE, Buckley CT. Investigating the physiological relevance of ex vivo disc organ culture nutrient microenvironments using in silico modeling and experimental validation. *JOR Spine*. 2021. doi:10.1002/jsp2.1141
113. Guehring T, Wilde G, Sumner M, et al. Notochordal intervertebral disc cells: Sensitivity to nutrient deprivation. *Arthritis Rheum*. 2009;60(4):1026-1034;
114. Cisewski SE, Wu Y, Damon BJ, Sachs BL, Kern MJ, Yao H. Comparison of Oxygen Consumption Rates of Nondegenerate and Degenerate Human Intervertebral Disc Cells. *Spine (Phila Pa 1976)*. 2018;43(2):E60-E67. doi:10.1097/BRS.0000000000002252
115. Razaq S, Wilkins RJ, Urban JPG. The effect of extracellular pH on matrix turnover by cells of the bovine nucleus pulposus. *Eur Spine J*. 2003;12(4):341-349;
116. Mwale F, Ciobanu I, Giannitsios D, Roughley PJ, Steffen T, Antoniou J. Effect of Oxygen Levels on Proteoglycan Synthesis by Intervertebral Disc Cells. *Spine (Phila Pa 1976)*. 2011;36(2):131-138. doi:10.1097/BRS.0b013e3181d52b9e
117. Naqvi SM, Buckley CT. Extracellular matrix production by nucleus pulposus and bone marrow stem cells in response to altered oxygen and glucose microenvironments. *J Anat*. 2015;227(6):757-766. doi:10.1111/joa.12305
118. Feng G, Li L, Liu H, et al. Hypoxia differentially regulates human nucleus pulposus and annulus fibrosus cell extracellular matrix production in 3D scaffolds. *Osteoarthr Cartil*.

2013;21(4):582-588. doi:10.1016/j.joca.2013.01.001

119. Chen JW, Li B, Yang YH, Jiang SD, Jiang LS. Significance of hypoxia in the physiological function of intervertebral disc cells. *Crit Rev Eukaryot Gene Expr*. 2014;24(3):193-204. doi:10.1615/CritRevEukaryotGeneExpr.2014010485
120. Bendtsen M, Bunger C, Colombier P, et al. Biological challenges for regeneration of the degenerated disc using cellular therapies. *Acta Orthop*. 2016;87:39-46. doi:10.1080/17453674.2017.1297916
121. Wills CR, Foata B, González Ballester MA, Karppinen J, Noailly J. Theoretical explorations generate new hypotheses about the role of the cartilage endplate in early intervertebral disk degeneration. *Front Physiol*. 2018;9(SEP):1-12. doi:10.3389/fphys.2018.01210
122. Bue M, Hanberg P, Thomassen MB, et al. Microdialysis for the Assessment of Intervertebral Disc and Vertebral Cancellous Bone. *In Vivo (Brooklyn)*. 2020;34(2):527-532. doi:10.21873/invivo.11804
123. Wang Y. Enhancement of Nutrient Transport and Energy Production of the Intervertebral Disc by the Implantation of Polyurethane Mass Transfer Device. 2017.
124. Fournier DE, Kiser PK, Shoemaker JK, Battié MC, Séguin CA. Vascularization of the human intervertebral disc: A scoping review. *JOR Spine*. 2020;(August):1-13. doi:10.1002/jsp2.1123
125. Fields AJ, Liebenberg EC, Lotz JC. Innervation of pathologies in the lumbar vertebral endplate and intervertebral disc. *Spine J*. 2014;14(3):513-521. doi:10.1016/j.spinee.2013.06.075.Innervation
126. Van Der Werf M, Lezuo P, Maissen O, Van Donkelaar CC, Ito K. Inhibition of vertebral endplate perfusion results in decreased intervertebral disc intranuclear diffusive transport. *J Anat*. 2007;211(6):769-774. doi:10.1111/j.1469-7580.2007.00816.x

127. Gullbrand SE, Peterson J, Mastropolo R, et al. Drug-induced changes to the vertebral endplate vasculature affect transport into the intervertebral disc in vivo. *J Orthop Res*. 2014;32(12):1694-1700. doi:10.1002/jor.22716

128. Benneker LM, Heini PF, Alini M, Anderson SE, Ito K. 2004 Young investigator award winner: Vertebral endplate marrow contact channel occlusions and intervertebral disc degeneration. *Spine (Phila Pa 1976)*. 2005;30(2):167-173; doi:10.1097/01.brs.0000150833.93248.09

129. Laffosse JM, Accadbled F, Molinier F, Bonnevialle N, De Gauzy JS, Swider P. Correlations between effective permeability and marrow contact channels surface of vertebral endplates. *J Orthop Res*. 2010;28(9):1229-1234. doi:10.1002/jor.21137

130. Krug R, Joseph GB, Han M, et al. Associations between vertebral body fat fraction and intervertebral disc biochemical composition as assessed by quantitative MRI. *J Magn Reson Imaging*. 2019. doi:10.1002/jmri.26675

131. Montazel JL, Divine M, Lepage E, Kobeiter H, Breil S, Rahmouni A. Normal Spinal Bone Marrow in Adults: Dynamic Gadolinium-enhanced MR Imaging. *Radiology*. 2003. doi:10.1148/radiol.2293020747

132. Gantenbein B, Calandriello E, Wuertz-Kozak K, Benneker LM, Keel MJB, Chan SCW. Activation of intervertebral disc cells by co-culture with notochordal cells, conditioned medium and hypoxia. *BMC Musculoskelet Disord*. 2014;15(1):1-15. doi:10.1186/1471-2474-15-422

133. Johnson ZI, Schoepflin ZR, Choi H, Shapiro IM, Risbud M V. Disc in flames: Roles of TNF-α and IL-1β in intervertebral disc degeneration. *Eur Cells Mater*. 2015;30:104-117. doi:10.22203/eCM.v030a08

134. Gilbert HTJ, Hodson NW, Baird P, Richardson SM, Hoyland JA. Acidic pH promotes intervertebral disc degeneration: Acid-sensing ion channel -3 as a potential therapeutic

target. *Sci Rep*. 2016;6(1):37360. doi:10.1038/srep37360

135. Le Maitre CL, Freemont AJ, Hoyland JA. The role of interleukin-1 in the pathogenesis of human intervertebral disc degeneration. *Arthritis Res Ther*. 2005;7(4):732-745. doi:10.1186/ar1732

136. Wuertz K, Vo N, Kletsas D, Boos N. Inflammatory and catabolic signalling in intervertebral discs: The roles of NF-KB and map kinases. *Eur Cells Mater*. 2012. doi:10.22203/ecm.v023a08

137. Le Maitre CL, Dahia CL, Giers M, et al. Development of a standardized histopathology scoring system for human intervertebral disc degeneration: an Orthopaedic Research Society Spine Section Initiative. *Jor Spine*. 2021;(June):1-29. doi:10.1002/jsp2.1150

138. Orozco L, Soler R, Morera C, Alberca M, Sánchez A, García-Sancho J. Intervertebral disc repair by autologous mesenchymal bone marrow cells: A pilot study. *Transplantation*. 2011;92(7):822-828. doi:10.1097/TP.0b013e3182298a15

139. Coric D, Pettine K, Sumich A, Boltes MO. Prospective study of disc repair with allogeneic chondrocytes. *J Neurosurg Spine J Neurosurg Spine*. 2013;18(18):85-95. doi:10.3171/2012.10.SPINE12512

140. Comella K, Silbert R, Parlo M. Effects of the intradiscal implantation of stromal vascular fraction plus platelet rich plasma in patients with degenerative disc disease. *J Transl Med*. 2017;15(1):4-11. doi:10.1186/s12967-016-1109-0

141. Kumar H, Ha DH, Lee EJ, et al. Safety and tolerability of intradiscal implantation of combined autologous adipose-derived mesenchymal stem cells and hyaluronic acid in patients with chronic discogenic low back pain: 1-year follow-up of a phase i study. *Stem Cell Res Ther*. 2017;8(1):1-14. doi:10.1186/s13287-017-0710-3

142. Sampson SL, Sylvia M, Fields AJ. Effects of dynamic loading on solute transport through the human cartilage endplate. *J Biomech*. 2019;83:273-279.

doi:10.1016/j.jbiomech.2018.12.004

143. Xiao ZF, He JB, Su GY, et al. Osteoporosis of the vertebra and osteochondral remodeling of the endplate causes intervertebral disc degeneration in ovariectomized mice. *Arthritis Res Ther*. 2018;20(1):207. doi:10.1186/s13075-018-1701-1